Received: 24 May 2018 | Revised: 19 November 2018 | Accepted: 4 January 2019 | Published on: 4 February 2019

DOI: 10.1002/joc.5991

International Journal of Climatology RMetS

RESEARCH ARTICLE

A quantile–quantile adjustment of the EURO-CORDEX projections for temperatures and precipitation

M.F. Cardell | R. Romero | A. Amengual | V. Homar | C. Ramis

Grup de Meteorologia, Departament de Física, Universitat de les Illes Balears, Palma de Mallorca, Spain

Correspondence
M. F. Cardell, Departament de Física, Universitat de les Illes Balears, 07122 Palma de Mallorca, Spain.
Email: maria.cardell@uib.es

Funding information
Conselleria d'Innovació, Recerca i Turisme del Govern de les Illes Balears, Grant/Award Number: FPI-CAIB (FPI/ 1931/ 2016); Secretaría de Estado de Investigación, Desarrollo e Innovación, Grant/ Award Number: CGL2014- 52199- R

Projections of climate change impacts over Europe are derived using a new quantile–quantile adjustment method. E-OBS high-resolution gridded data sets of daily observed precipitation and 2-m surface minimum and maximum temperatures have been used as the current climate baseline. For projections, the same meteorological variables have been obtained from a set of regional climate models (RCMs) integrated in the EURO-CORDEX project, and by considering the RCP4.5 and RCP8.5 future emissions scenarios. To enhance the reliability of RCM data at local scale, new developments of a previous quantile–quantile adjustment have been applied to the simulated regional scenarios. This method focuses not only on the bulk spectrum of the cumulative distribution functions but also on its tails. Results show an overall improvement in reproducing the present climate baseline when using calibrated series instead of raw RCM outputs. Next, we have used these locally adjusted series to quantify the climate change signal through a number of annual and seasonal indicators. A significant increase of the minimum and maximum temperatures in all seasons is projected over Europe, being more marked in the Mediterranean for summer and autumn. Prospects on future seasonal and annual changes in precipitation are more diverse, showing an overall decrease in southern Europe and the Mediterranean, while precipitation is expected to increase towards the north of the continent. With these sources of information at hand, including and accounting for the identification of the most vulnerable geographical areas, policy makers and stakeholders can respond more effectively to the future challenges imposed by climate change.

KEYWORDS
climate change, precipitation, quantile–quantile adjustment, regional climate models, temperatures

1 | INTRODUCTION

Climate change is one of the major challenges faced by our societies owing to the potential implications on health, environment and economy, among other sectors. Observations show that global mean surface air temperatures over land and oceans have notably increased over the last 100 years. In fact, 1983–2012 was likely the warmest 30-year period of the last 1,400 years in the Northern Hemisphere (Stocker *et al*., 2013). The average global temperature increased by 0.85 °C from 1880 to 2012. Associated with this global warming, a redistribution of rainfall and other atmospheric variables (e.g., pressure, cloudiness, wind) has been observed with even higher spatial variability than for temperature. Europe emerges as an especially responsive area to this temperature rise, particularly during the warm season (Giorgi, 2006). Furthermore, projections indicate that it is very likely that temperatures will continue to increase throughout the 21st century over all of Europe and the Mediterranean region, while

precipitation will be more variable across subregions and seasons (Stocker *et al*., 2013).

In terms of future projections, atmosphere–ocean general circulation models (GCMs) have been widely used to study global and continental changes. GCM simulations have been run under a wide range of scenarios for greenhouse gas emissions and aerosols (representative concentration pathways [RCPs] scenarios) (Moss *et al*., 2008). These scenarios describe plausible evolutions of the emissions depending on socioeconomic development and climate policy (Amengual *et al*., 2012). Even though these models are adequate to provide future global climate scenarios, their current resolution is not suitable to deal directly with local climates and extreme phenomena. In addition, they poorly incorporate local effects associated with complex topography and are unable to explicitly resolve some of the responsible atmospheric circulations. Therefore, different downscaling techniques are applied on GCM's outputs in order to obtain reliable climate change information at regional to local scales. Dynamical downscaling using a regional climate model (RCM) is an example of such a technique.

RCMs (Giorgi and Mearns, 1999; Wang *et al*., 2004) are widely used tools for providing regional climate information over limited areas. In the last decade, there has been a rapid growth in the availability and reliability of RCM simulations for Europe, thanks to projects such as PRUDENCE (Christensen and Christensen, 2007), ENSEMBLES (Van der Linden and Mitchell, 2009), STARDEX (Goodess *et al*., 2012), and more recently, CORDEX (Giorgi *et al*., 2009). However, since RCM outputs suffer from systematic errors (simple parameterizations, still too coarse spatial resolution, etc.) it is advisable to correct them to obtain meaningful results on the simulated properties of the climate system (Štěpánek *et al*., 2016). The issue is aggravated when daily data and extreme values are analysed, since incorrect statistical distributions simulated by a model for a given meteorological variable may lead to wrong conclusions. Although RCMs often improve the performance of GCMs at regional scales, their used spatial resolutions still remain inadequate to address uncertainties emerging from different sources (e.g., local topographic forcing, sea–land transition along complex coasts, urban effects, etc.). We present an improvement upon the statistical correction method of (Amengual *et al*., 2012) that conducts a quantile–quantile (Q–Q) adjustment of climate model outputs. The improved method is applied to several projections of temperature and precipitation by EURO-CORDEX RCMs to better assess climate change impacts over Europe.

As a successor of past projects like ENSEMBLES and PRUDENCE, the CORDEX (Coordinated Regional Climate Downscaling Experiment) initiative (Giorgi *et al*., 2009) aims to supply an internationally coordinated framework to compare, enhance and standardize regional climate downscaling methods, covering both dynamical and empirical–statistical approaches (Kotlarski *et al*., 2014). EURO-CORDEX, the European contribution to the CORDEX initiative (Jacob *et al*., 2014), produces regional climate scenarios for Europe at grid resolutions of about 12 and 50 km, which are based on different RCPs (Moss *et al*., 2008). These scenarios take radiative forcing (W/m^2) as the characteristic driving variable, instead of the concentration of the equivalent CO_2 (ppm) (Štěpánek *et al*., 2016). The present work focuses on the RCP4.5 and RCP8.5 scenarios since they represent an intermediate stabilization pathway and the more pessimistic pathway of greenhouse emissions, respectively. Emissions in RCP4.5 are expected to reach the maximum around 2040, and then decline, while in RCP8.5, emissions continue to increase throughout the 21st century (Meinshausen *et al*., 2011).

The structure of the paper is as follows: section 2 describes the observations and simulations databases, and the proposed empirical correction method along with the new improvements and validation test of the technique; section 3 discusses the projected annual and seasonal mean changes for the parameters of interest; finally, section 4 summarizes the main results and conclusions, offering some additional remarks for future work.

2 | DATABASE AND METHODS

2.1 | Input data

The observational references used in this study were obtained from the E-OBS data set (Haylock *et al*., 2008) that was developed within the EU-funded Project ENSEMBLES. It is known for its extensive use in regional climate model evaluation, among many other applications (Herrera *et al*., 2016). E-OBS covers the entire European land surface and is based on the European Climate Assessment and Dataset station data set (ECA&D) with more than 2,000 stations from different sources (Kotlarski *et al*., 2014). The observational database has four different resolutions: here we use the highest available in E-OBS (0.22°), which corresponds to a horizontal resolution of about 25 km and uses the same grid rotation as most of the ENSEMBLES and EURO-CORDEX simulations. According to recent studies, E-OBS tends to underestimate mean precipitation in some regions of Europe (e.g., south of Spain, the Alpine region), specially during summer and winter (Kotlarski *et al*., 2017). Therefore, RCM simulations calibrated using the E-OBS database as reference climate would also underestimate the future mean precipitation in these regions, but the general pattern of changes should not be significantly affected.

In order to build our method to assess future climate change, present-climate reference data consisting of daily series of 2-m minimum and maximum temperatures and accumulated daily precipitation for the 1981–2005 period (25 years) have been used. Additionally, the same kind of

data for the past period 1956–1980 was handled for the validation task of section 2.3.

Regarding the future projections, we use the regional simulations available from the EURO-CORDEX project (http://www.euro-cordex.net). A set of 14 RCM simulations of daily series of 2-m minimum and maximum temperatures and accumulated precipitation has been obtained (Table 1). In total, we count on five RCMs at grid resolutions of about 12 km driven by different GCMs under the future scenarios RCP4.5 and RCP8.5. All simulations cover the 1950–2100 period. From this, 1981–2005 has been selected as the present period so as to apply the quantile–quantile adjustment. The 2005–2100 interval is used to assess climate change impacts. This future period has been divided in three successive 25-year time slices, from 2021 to 2095, in order to analyse the climate change signal in section 3.

2.2 | Quantile–quantile adjustment method

There are several procedures to correct RCM projections, taking local forcings into consideration. Two simple corrections are based on (a) adding the climatological difference between the future and control climate scenario simulations to an observed baseline (the "delta-change" method) and (b) removing the bias from future simulations by applying the climatological difference between the observed and control data (the un-biasing method; Déqué, 2007). There are two important assumptions associated with these techniques; in the former approach, the variability in the climate scenario remains unchanged, and in the latter proposal, RCM variability is considered perfect (Amengual *et al*., 2012).

Adjustments of the whole climatic distribution through quantile-mapping techniques have been widely used as they allow to adjust not only the mean and variance but also any quantile of the variable of interest. Therefore, several methods have been proposed (e.g., Reichle and Koster, 2004; Wood *et al*., 2004; Boé *et al*., 2007; Déqué, 2007; Dobler and Ahrens, 2008; Piani *et al*., 2010; Johnson and Sharma, 2012; Suh *et al*., 2012; Teutschbein and Seibert, 2012; Themeßl *et al*., 2012; Ahmed *et al*., 2013; Tramblay *et al*., 2013; Cannon *et al*., 2015; Vrac *et al*., 2016; Ivanov and Kotlarski, 2017). The quantile–quantile correction methodology has three main limitations to be considered (Boé *et al*., 2007): the temporal autocorrelation properties of the series are not corrected (e.g., wet spells in the RCM may still exist after the correction); second, each variable is corrected independently, whereas for instance, bias in precipitation might not be independent of bias in temperature; finally, climate model outputs have a strong spatial autocorrelation which may be biased. Recent studies deal with the characterization of the above limitations (Maraun *et al*., 2017), while other authors address the need for methods adjusting not only the marginal distributions of the climate simulations but also their multivariate dependence structures (e.g., Ivanov *et al*., 2018; Vrac, 2018).

Within this context, we devise a modified version of the statistical method presented by Amengual *et al*. (2012), specifically focused to ameliorate the extremes of the distribution. This method is founded on a nonparametric function that amends mean, variability, and shape errors in the simulated cumulative distribution functions (CDFs) of the climatic variables.

It can be expressed as the following relationship between the *i*th ranked value p_i (projected or future calibrated), o_i (control observed or baseline), s_{fi} (raw future simulated), and s_{ci} (raw control simulated), of the corresponding CDFs (Figure 1),

$$p_i = o_i + \alpha\bar{\Delta} + \beta\Delta_i^{'}, \tag{1}$$

where

$$\Delta_i = s_{fi} - s_{ci}, \tag{2}$$

$$\bar{\Delta} = \frac{\sum_{i=1}^{N}\Delta_i}{N} = \frac{\sum_{i=1}^{N}\left(s_{fi} - s_{ci}\right)}{N} = \bar{S_f} - \bar{S_c}, \tag{3}$$

$$\Delta_i^{'} = \Delta_i - \bar{\Delta}, \tag{4}$$

$$\alpha = \frac{\left(\sum_{i=1}^{N} o_i\right)/N}{\left(\sum_{i=1}^{N} s_{ci}\right)/N} = \frac{\bar{O}}{\bar{S_c}}, \tag{5}$$

$$\beta = \frac{\sigma_O}{\sigma_{S_c}}. \tag{6}$$

The σ_O and σ_{S_c} in Equation 6 are the interquartile ranges of the observed and raw control simulated data, respectively, that is, the parametric difference between 75th (P75) and 25th (P25) percentiles for temperatures. However, for precipitation we used the 90th (P90) and 10th (P10) percentiles due to the highly asymmetrical gamma-type distribution of the variable, with a high

TABLE 1 List of RCM experiments performed within the EURO-CORDEX project for the 1950–2100 period. Note that all models have a spatial resolution of 12 km and have been run under the RCP4.5 and RCP8.5 future scenarios

Institute	Driving GCM	RCM
CNRM	CNRM-CM5-LR	ALADIN53
CLMcom	CNRM-CM5-LR	CCLM4-8-17
CLMcom	EC-EARTH	CCLM4-8-17
CLMcom	HadGEM2-ES	CCLM4-8-17
CLMcom	CNRM-CM5-LR	CCLM4-8-17
DMI	EC-EARTH	HIRHAM5
DMI	NorESM1-M	HIRHAM5
KNMI	EC-EARTH	RACMO22E
KNMI	EC-EARTH	RACMO22E
SMHI	CNRM-CM5-LR	RCA4
SMHI	EC-EARTH	RCA4
SMHI	HasGEM2-ES	RCA4
SMHI	MPI-ESM-LR	RCA4
SMHI	IPSL-CM5A-MR	RCA4

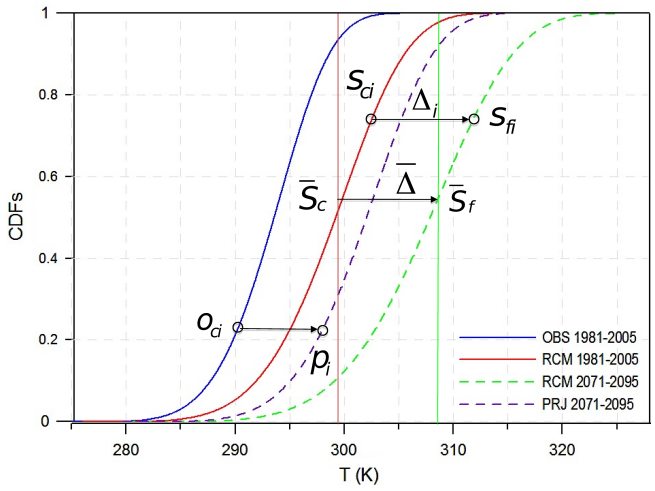

FIGURE 1 Graphical sketch of the Q–Q adjustment. The CDFs of the mean temperatures are shown for the observed control (OBS 1981–2005), raw control (RCM 1981–2005), and future simulated (RCM 2071–95) and calibrated or projected (PRJ 2071–2095) data. The statistical correction is illustrated between the 25-year past (1981–2005) and future (2071–2095) periods. Vertical lines denote mean values for raw control ($\bar{S}_c$) and future ($\bar{S}_f$) simulated periods [Colour figure can be viewed at wileyonlinelibrary.com]

proportion of non-rainy days. In the equations, Δ_i is the difference between future and control raw *i*th quantiles (Figure 1). Accordingly, it can be written as the sum of the mean regime shift ($\bar{\Delta}$) plus the corresponding deviation Δ'_i from this shift (Equations 2–4).

The variation in the mean state $\bar{\Delta}$ is modulated by α (the scale factor), while β (the form factor) calibrates the change in variability and shape expressed by Δ'_i. The α and β parameters are used to reconcile the RCM in the control period with the observed climate: a parameter value greater (smaller) than 1 would act to inflate (deflate) an otherwise too low (high) contribution to the change of the corresponding climate attribute. The form factor is used for all variables (minimum temperature, maximum temperature, and precipitation) while the scale factor is not applied for temperatures (i.e., $\alpha = 1$). This means that changes in the modelled temperatures mean states are counted in absolute terms ($\bar{\Delta}$), while for the precipitation, relative changes are employed instead, as widely applied in the climate literature (see Amengual *et al*., 2012, appendix).

This previous method, hereinafter the *global* calibration approach, has been slightly adapted to focus not only on the gross features of the distributions (as described by σ_O and σ_{S_c} in Equation 6) but on all ranges of values, including the tails of the distributions. Specifically, β that determines the adjustment of variability and shape of the distribution has been modified to acquire a local character (β_i). The new method is labelled as *local* calibration since now the form

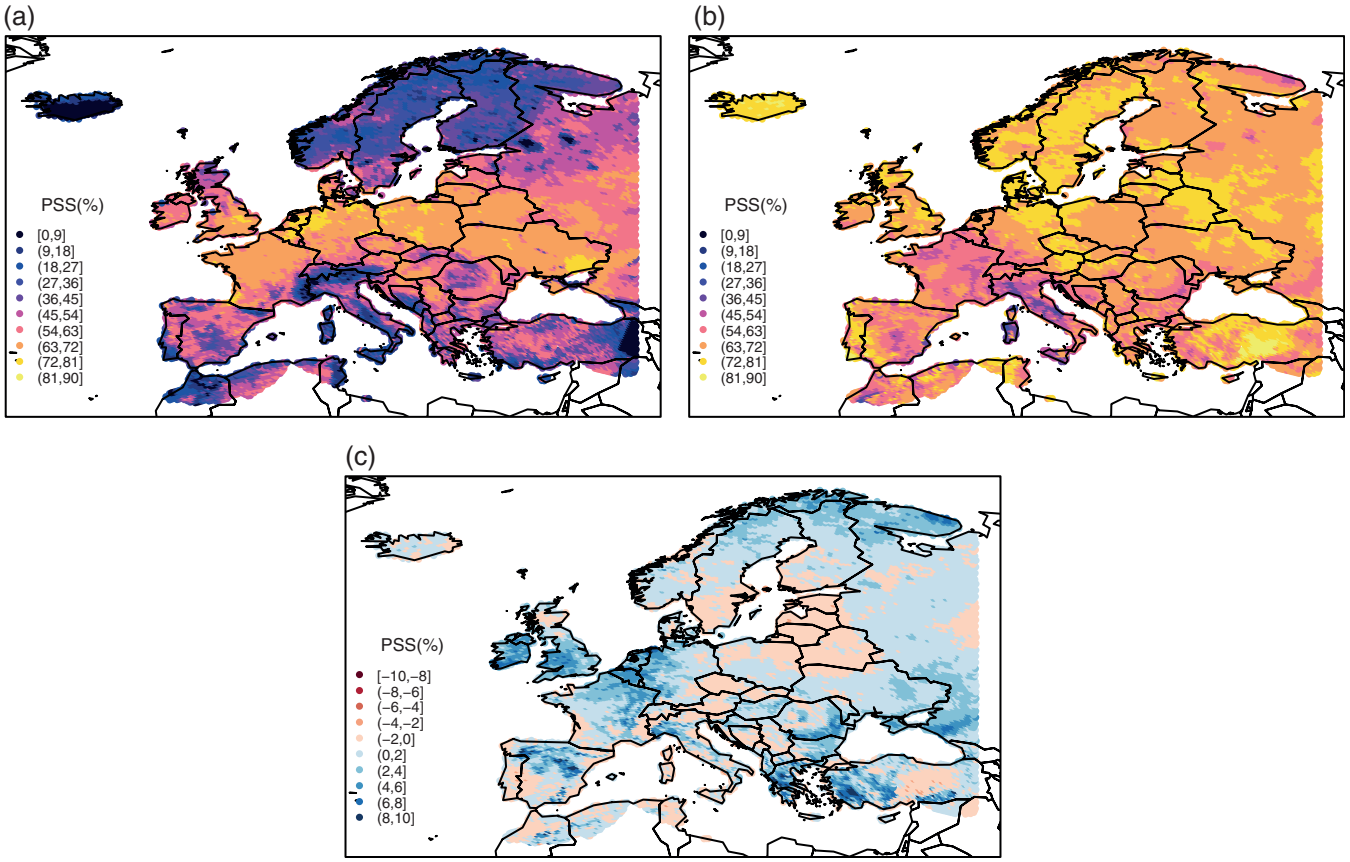

FIGURE 2 PSS (%, model's ensemble mean) under fifth percentile for minimum temperature in winter between (a) the raw and observed PDFs and (b) the global calibrated and observed PDFs. (c) Difference between the PSS (%, model's ensemble mean) of local-observed PDFs and global-observed PDFs [Colour figure can be viewed at wileyonlinelibrary.com]

TABLE 2 Multi-model mean areal average PSS (%) for the 1956–1980 raw, *global*, and *local* calibrated PDFs for the indicated atmospheric parameters (largest value emphasized in bold). Also shown the standard deviation between models. Note that summer results for precipitation are not considered since this season is fully dry in many zones of the domain

Precipitation (mm)		**Annual**	**Winter**	**Spring**	**Summer**	**Autumn**
Whole PDF	Raw	**86.5** ± 3.0	**84.6** ± 4.5	**81.9** ± 5.7		78.2 ± 5.2
	Global	85.8 ± 2.7	81.8 ± 3.8	79.3 ± 4.1		79.0 ± 4.5
	Local	85.7 ± 2.4	81.7 ± 3.8	79.2 ± 4.0		79.0 ± 4.4
Over P_{95}	Raw	75.2 ± 9.1	66.3 ± 12.6	68.1 ± 11.0		72.2 ± 10.2
	Global	83.2 ± 5.1	74.2 ± 8.8	75.4 ± 9.6		75.2 ± 9.3
	Local	**84.1** ± 3.8	**75.1** ± 7.9	**76.6** ± 7.4		**77.1** ± 7.3
Over P_{99}	Raw	62.0 ± 15.5	51.1 ± 16.8	50.3 ± 15.6		55.4 ± 15.6
	Global	71.3 ± 8.7	57.6 ± 15.6	58.4 ± 16.2		57.2 ± 16.2
	Local	**73.4** ± 9.0	**58.6** ± 14.7	**60.1** ± 14.1		**59.8** ± 14.2
Min. temperature (°C)		**Annual**	**Winter**	**Spring**	**Summer**	**Autumn**
Whole PDF	Raw	83.3 ± 8.1	78.2 ± 14.5	78.8 ± 12.2	75.1 ± 7.3	83.6 ± 8.5
	Global	93.6 ± 2.0	**86.8** ± 11.2	89.8 ± 3.3	91.3 ± 3.4	**91.5** ± 2.4
	Local	**93.6** ± 1.9	86.8 ± 11.2	**89.8** ± 3.2	**91.4** ± 3.3	91.4 ± 2.5
Under P_5	Raw	60.9 ± 19.7	49.5 ± 22.9	52.0 ± 22.4	36 ± 27.9	57.2 ± 18.8
	Global	75.9 ± 10.1	62.4 ± 18.6	64.8 ± 15.7	71.2 ± 14.1	**68.5** ± 12.3
	Local	**76.5** ± 9.6	**63.6** ± 17.0	**65.0** ± 15.2	**71.2** ± 14.0	68.0 ± 12.6
Over P_{95}	Raw	46.1 ± 26.4	47.2 ± 26.3	43.4 ± 28.0	35.4 ± 26.9	50.4 ± 23.7
	Global	77.1 ± 9.8	64.8 ± 22.7	70.3 ± 13.5	65.8 ± 14.7	71.4 ± 12.6
	Local	**77.5** ± 9.6	**65.7** ± 21.0	**71.0** ± 12.7	**66.8** ± 14.1	**72.0** ± 12.1
Max. temperature (°C)		**Annual**	**Winter**	**Spring**	**Summer**	**Autumn**
Whole PDF	Raw	85.1 ± 5.8	76.9 ± 15.4	81.0 ± 9.0	75.5 ± 15.3	85.9 ± 5.6
	Global	94.4 ± 1.7	85.5 ± 14.7	91.2 ± 3.0	90.9 ± 3.3	**91.9** ± 2.6
	Local	**94.5** ± 1.7	**85.6** ± 14.6	**91.2** ± 3.0	**90.9** ± 3.3	91.8 ± 2.5
Under P_5	Raw	62.5 ± 15.4	51.8 ± 19.6	49.9 ± 21.2	44.8 ± 23.7	53.2 ± 16.7
	Global	77.3 ± 9.3	62.8 ± 17.7	62.8 ± 17.3	71.7 ± 13.2	66.1 ± 13.2
	Local	**77.9** ± 8.8	**64.1** ± 16.3	**64.6** ± 15.4	**71.9** ± 13.0	**66.4** ± 13.0
Over P_{95}	Raw	44.4 ± 22.3	38.0 ± 23.5	39.7 ± 23.0	33.5 ± 23.3	51.2 ± 21.9
	Global	76.9 ± 9.9	63.3 ± 23.7	69.1 ± 13.0	65.6 ± 15.5	70.6 ± 13.4
	Local	**77.4** ± 9.8	**63.5** ± 23.5	**69.6** ± 12.6	**66.6** ± 14.9	**71.4** ± 12.7

factor changes in every part of the distribution, rather than being a constant extracted from the general spectrum of the CDF. In the following expression, $o_i^{'}$ and $s_{c_i}^{'}$ are the parametric differences between the observed *i*th quantile and its mean ($\bar{O}$), and the simulated *i*th quantile and its mean ($\bar{S_c}$), respectively,

$$\beta_i = \frac{o_i^{'}}{s_{c_i}^{'}} = \frac{o_i - \bar{O}}{s_{c_i} - \bar{S_c}}. \quad (7)$$

Additionally, the probability of precipitation in the simulations would be unrealistic since RCMs tend to overestimate the number of days with trace values, but also to underestimate the number of non-rainy days. To overcome this problem, a further restriction is imposed when applying the Q–Q correction to daily precipitation: the ratio of non-rainy days between future and control simulated raw data is imposed for the calibrated versus observed series, that is,

$$nz_p = \frac{nz_{s_f}}{nz_{s_c}} nz_o, \quad (8)$$

where nz_p, nz_o, nz_{s_c}, and nz_{s_f} are the number of zero-precipitation in the projected, observed, simulated control, and simulated future series, respectively.

2.3 | Validation of the local quantile–quantile adjustment technique

A validation of the new local Q–Q adjustment has been carried out so as to test the benefits of the statistical approach to enhance the representativity of the RCM data at local scale. The Q–Q adjustment consists of calculating the changes, quantile by quantile, in the CDFs of daily RCM outputs between a 25-year control period and successive 25-year future time slices (Figure 1). These changes are rescaled on the basis of the observed CDF for the same control period, and then added, quantile by quantile, to these observations to obtain new calibrated future CDFs that convey the climate change signal. Periods of 25-year have been chosen owing to the temporal limitation of the observed database (50 year): we have divided the daily series into an early

TABLE 3 As in Table 2, but for *alternate* years 1956–2005

Precipitation (mm)		**Annual**	**Winter**	**Spring**	**Summer**	**Autumn**
Whole PDF	Raw	86.4 ± 4	24.1 ± 4.5	**80.8** ± 6.2		78.5 ± 5.3
	Global	86.5 ± 3.2	**82.5** ± 3.2	79.2 ± 4.7		79.0 ± 4.6
	Local	**86.5** ± 2.0	82.2 ± 3.4	79.1 ± 3.0		79.0 ± 4.2
Over P_{95}	Raw	75.4 ± 9.1	67.9 ± 12.1	67.5 ± 11.1		71.9 ± 10.0
	Global	78.8 ± 5.1	78.2 ± 7.8	76.2 ± 9.1		75.6 ± 9.6
	Local	**86.0** ± 3.2	**78.9** ± 7.0	**77.4** ± 7.1		**77.3** ± 7.1
Over P_{99}	Raw	62.5 ± 12.7	51.8 ± 16.4	50.0 ± 15.1		55.6 ± 15.1
	Global	68.5 ± 10.0	60.9 ± 14.8	58.8 ± 15.8		58.7 ± 16.1
	Local	**76.0** ± 7.4	**61.9** ± 13.8	**60.5** ± 14.0		**60.9** ± 14.1
Min. temperature (°C)		**Annual**	**Winter**	**Spring**	**Summer**	**Autumn**
Whole PDF	Raw	83.7 ± 8.0	80.4 ± 11.0	79.7 ± 11.9	75.7 ± 15.0	83.9 ± 8.1
	Global	95.0 ± 1.5	90.8 ± 3.2	**91.1** ± 2.6	**93.1** ± 2.4	91.7 ± 2.8
	Local	**95.1** ± 1.5	**91.0** ± 3.0	91.0 ± 2.6	93.0 ± 2.4	**91.7** ± 2.7
Under P_5	Raw	61.4 ± 19.7	50.2 ± 21.5	50.5 ± 23.0	35.7 ± 27.8	56.5 ± 19.5
	Global	82.4 ± 8.1	67.2 ± 14.2	**72.9** ± 11	75.0 ± 12.3	**67.3** ± 13.3
	Local	**82.7** ± 7.5	**68.3** ± 13.2	72.7 ± 10.7	**75.2** ± 11.9	67.0 ± 12.9
Over P_{95}	Raw	51.2 ± 26.6	51.4 ± 22.8	46.0 ± 26.7	36.6 ± 27.1	51.0 ± 23.6
	Global	82.1 ± 7.7	72.7 ± 11.1	69.4 ± 12.6	72.0 ± 12.7	75.0 ± 11.0
	Local	**82.5** ± 7.5	**73.9** ± 10.2	**70.0** ± 12.1	**73.0** ± 12.0	**75.7** ± 10.3
Max. temperature (°C)		**Annual**	**Winter**	**Spring**	**Summer**	**Autumn**
Whole PDF	Raw	83.3 ± 5.6	79.6 ± 7.8	81.1 ± 8.6	76.2 ± 11.3	86.8 ± 5.8
	Global	95.1 ± 1.5	87.1 ± 15.1	91.6 ± 2.8	**92.9** ± 2.4	92.1 ± 2.9
	Local	95.1 ± 1.5	**90.8** ± 2.9	**91.7** ± 2.8	92.8 ± 2.4	**92.2** ± 3.0
Under P_5	Raw	61.5 ± 15.4	50.8 ± 20.0	44.2 ± 21.8	45.1 ± 23.7	54.2 ± 16.1
	Global	**83.3** ± 8.1	67.9 ± 13.9	68.5 ± 13.4	75.1 ± 11.9	65.3 ± 16.1
	Local	83.0 ± 7.7	**69.0** ± 13.1	**69.4** ± 12.5	**75.3** ± 11.7	**66.1** ± 15.0
Over P_{95}	Raw	49.9 ± 22.3	39.6 ± 20.8	40.9 ± 23.6	35.1 ± 24.3	53.0 ± 21.9
	Global	81.4 ± 8.1	66.7 ± 22.2	69.5 ± 13.4	70.7 ± 13.2	73.1 ± 12.4
	Local	**81.6** ± 7.9	**72.2** ± 10.4	**69.9** ± 13.0	**71.5** ± 12.6	**74.0** ± 11.6

period for the validation purposes (1956–1980) and a later interval for the calibration task (1981–2005; control or baseline).

For the validation process, we first evaluated the performance of the multi-model for the above 25-year period (1956–1980) by comparing the raw and calibrated data percentiles against the observations. A second validation of the technique was performed, this time for a period of 25 *alternate* years from 1956 to 2004, with the goal to mitigate the effects of the climate change signal, already present throughout the historical study period. In this study, we are interested in analysing not only the annual changes in mean regimes but also the seasonal shifts, which may present singular behaviours in particular zones compared to annual tendencies. For this purpose, the statistical correction approach was carried out seasonally and subsequently an aggregation was made to analyse the results at annual scale.

The method followed to achieve the validation task consists of evaluating the Perkins skill score (PSS; Perkins *et al.*, 2007), a very simple but rather useful measure of the overlap between two probability density functions (PDFs). This measure of the common area between two PDFs, provides a skill score that will equal 1 when the modelled and observed PDFs are identical and 0 when there is not overlap at all. We analyse for the validation periods (*continuous* years and *alternate* years) the PSS between the raw and observed PDFs, as well as the PSS between the calibrated and observed PDFs.

Figure 2 shows an example of the ensemble mean PSS under the fifth percentile for the minimum temperature in winter and for the period of 25 *alternate* years from 1956 to 2004. There is an overall enhancement in the similarity between the models and the observations when we use the calibrated versus the uncalibrated data. The PSS spatial mean reveals a 50.2% overlap between the observed and raw simulated PDFs, with the highest values of PSS in the central part of Europe (Figure 2a). The PSS is significantly better if the calibrated (*global* method) and observed PDFs are compared (67.2%; Figure 2b) and slightly higher (68.3%) if the *local* method is used (Figure 2c). Note how the PSS notably increases in some regions (northern countries and Turkey) when the Q–Q adjustment is performed, although some deterioration can be also produced by the calibration in limited areas (e.g., northern France). Therefore, we expect

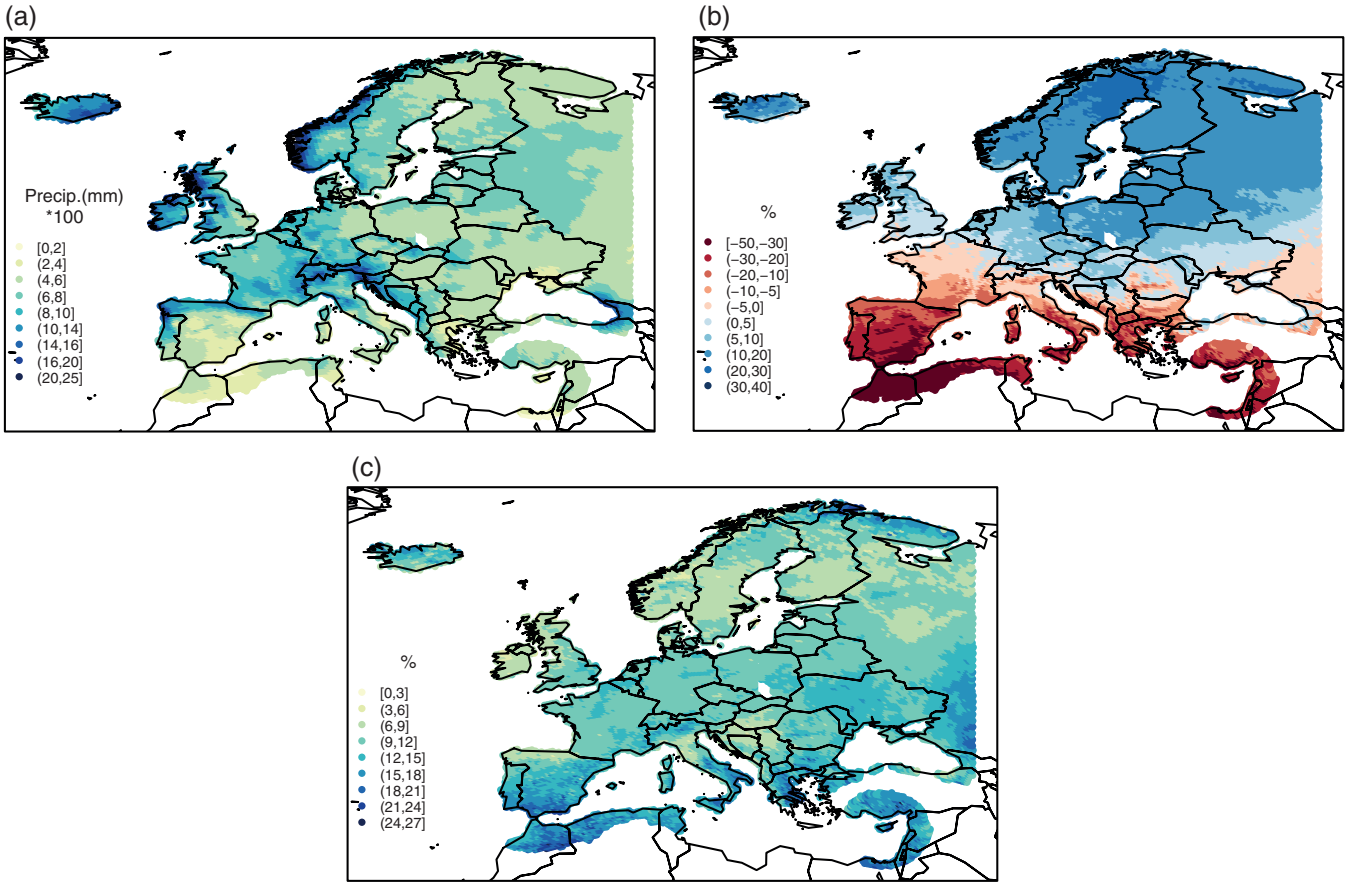

FIGURE 3 (a) Observed average annual precipitation, (b) future change (in %, multi-model mean, 2071–2095, RCP8.5), and (c) the inter-model *SD* of the change (in %) [Colour figure can be viewed at wileyonlinelibrary.com]

that our method generally corrects some of the systematic errors within RCMs and provides more meaningful results on the simulated climatic variables.

The PSS ensemble mean corresponding to the whole PDFs for daily precipitation, minimum and maximum daily temperature has been calculated to assess the overall performance of the method in both validation periods. The PSS associated to the tails of the distributions has also been computed (i.e., under 5th and over 95th percentiles) to evaluate the performance for extreme regimes. As the representation of very low intensity precipitation events in E-OBS is uncertain and does not allow a clear definition of rainy days (Kotlarski *et al*., 2017), the whole distribution has been used to define the precipitation extremes. This choice could question the definition of an extreme based on the 95th percentile over dry areas (Schär *et al*., 2016). To alleviate this misrepresentation, we will also include the 99th percentile value in the case of precipitation. In addition to the annual computations, the same validation procedure has been applied to winter (DJF), spring (MAM), summer (JJA), and autumn (SON).

Tables 2 and 3 display the results of the areal average Perkins skill score (multi-model mean) comparing the raw and calibrated PDFs against the observations for the validation periods. The results of the PSS using an interval of *continuous* years (1956–1980) has been analysed in Table 2, while those corresponding to the validation with *alternate* years (1956–2005) are shown in Table 3. In both cases, PSS reveals an evident improvement of the calibrated versus uncalibrated PDFs for all the atmospheric parameters, with the occasional exception of the precipitation for the whole PDF, where the PSS index between the raw and the observed distributions is slightly higher than the PSS of the calibrated and observed PDFs.

In summary, the net result of applying the calibration is clearly beneficial and the expected value of the PSS is generally higher when applying the new *local* adjustment. Specifically, the application of the *local* quantile–quantile adjustment clearly amends the errors found in the statistical distributions of the extreme values. The validation with *alternate* years (Table 3) also reveals a slightly better overlap between the calibrated and observed PDFs for all variables, both annually and seasonally. Therefore, it should be expected a certain level of degradation of the benefits of the Q–Q corrections if a significant climate change signal is accumulated between historical and future periods, as it is expected under high emission scenarios. Finally, the uncertainty range associated with the inter-model differences is also reduced by the adjustment, with the minimum standard deviation (*SD*) obtained when applying the *local* calibration adjustment.

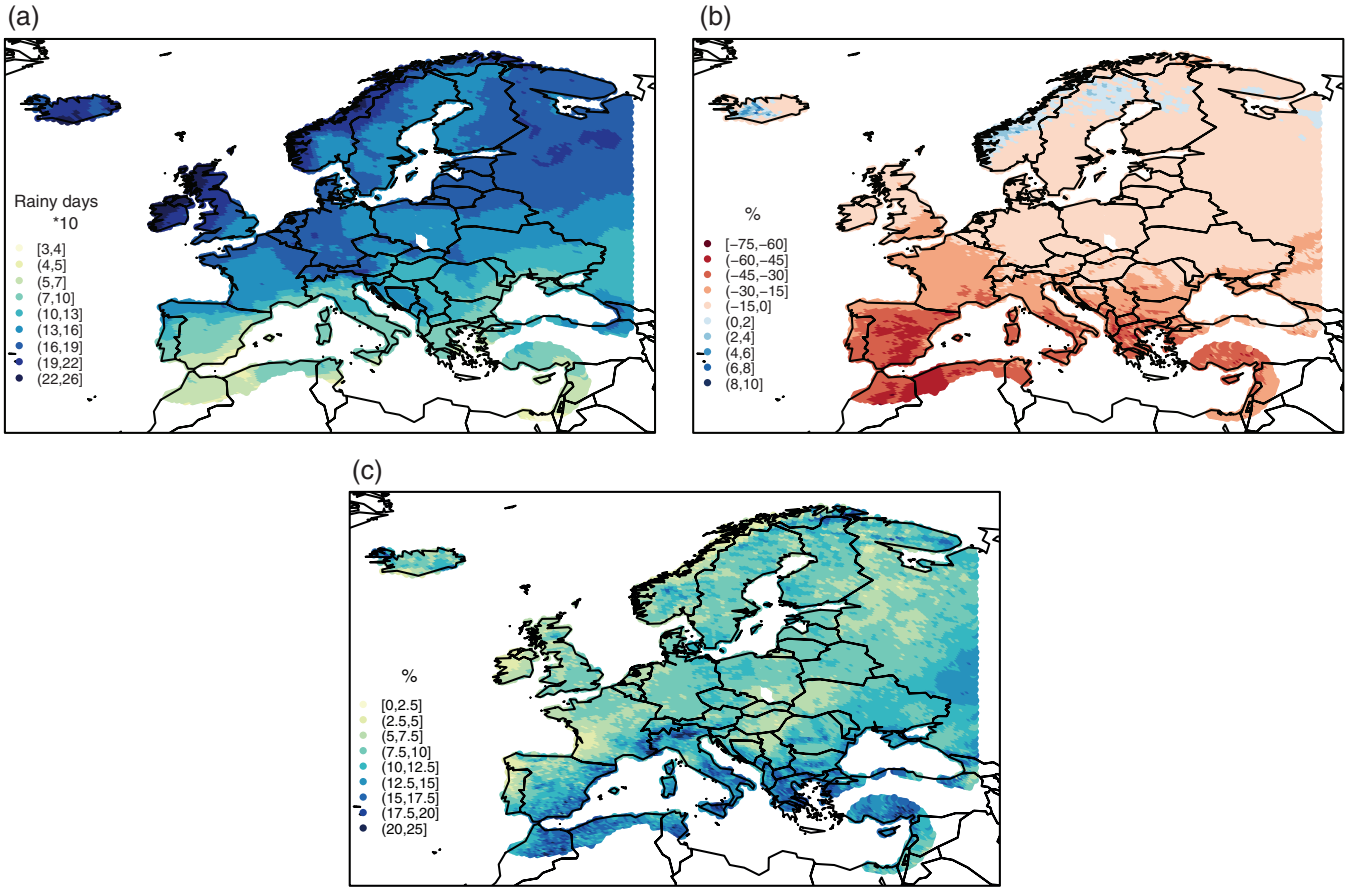

FIGURE 4 (a) Observed annual number of rainy days, (b) future change (in %, multi-model mean, 2071–2095, RCP8.5), and (c) the inter-model *SD* of the change (in %) [Colour figure can be viewed at wileyonlinelibrary.com]

Additional standard metrics like the quantile-wise mean absolute (MAE) and root mean square (RMSE) errors have been calculated for both the *continuous* and *alternate* validation samples, leading to the same conclusions pointed out by the PSS metric. Specifically, MAE and RMSE scores reveal an overall improvement for both mean and extreme regimes of the calibrated versus uncalibrated CDFs, and both indices are generally lowered when applying the *local* adjustment (tables not shown).

We have also carried out an inter-comparison between the *local* Q–Q adjustment presented in this work and the classical scheme used by Boé *et al.* (2007), denoted herein as *qmap* method, so as to test the benefits of the proposed approach. To illustrate the differences between both approaches, we computed for *qmap* the same PSS-based products as those shown in Tables 2 and 3. The validation with *alternate* years shows that the scores are practically equivalent between the *local* adjustment and the classic *qmap* for all seasons and daily atmospheric variables (tables not shown). Results for *continuous* years are quite similar in many cases but when the *qmap* PSS is worse than the *local* approach, the performance is clearly lower, especially for extreme values (e.g., PSS above P95 in winter). This behaviour may be a consequence of the use of a simple extrapolation of the *qmap* method when daily variables in the simulated climate scenario exceed the greatest value found in the reference period (Boé *et al.*, 2007).

3 | RESULTS AND DISCUSSION

3.1 | Future changes in annual precipitation

Once RCM raw outputs have been statistically adjusted within the European domain, the climate change signal has been analysed by studying changes obtained from 1981–2005 (observed time slice, present) and the multi-model ensemble means of three future 25-year time slices: 2021–2045 (early 21st century), 2046–2070 (mid-21st century), 2071–2095 (late 21st century). For the sake of brevity, we will focus the discussion and graphical displays on the expected changes during the late 21st century under the RCP8.5 emission scenario. Undoubtedly, this seems to be the most likely emissions pathway in the next decades, unless strict greenhouse gas mitigation policies are implemented.

Figure 3a,b depicts the observed mean annual precipitation and the future change (multi-model mean) respectively, together with the associated uncertainty (Figure 3c). An

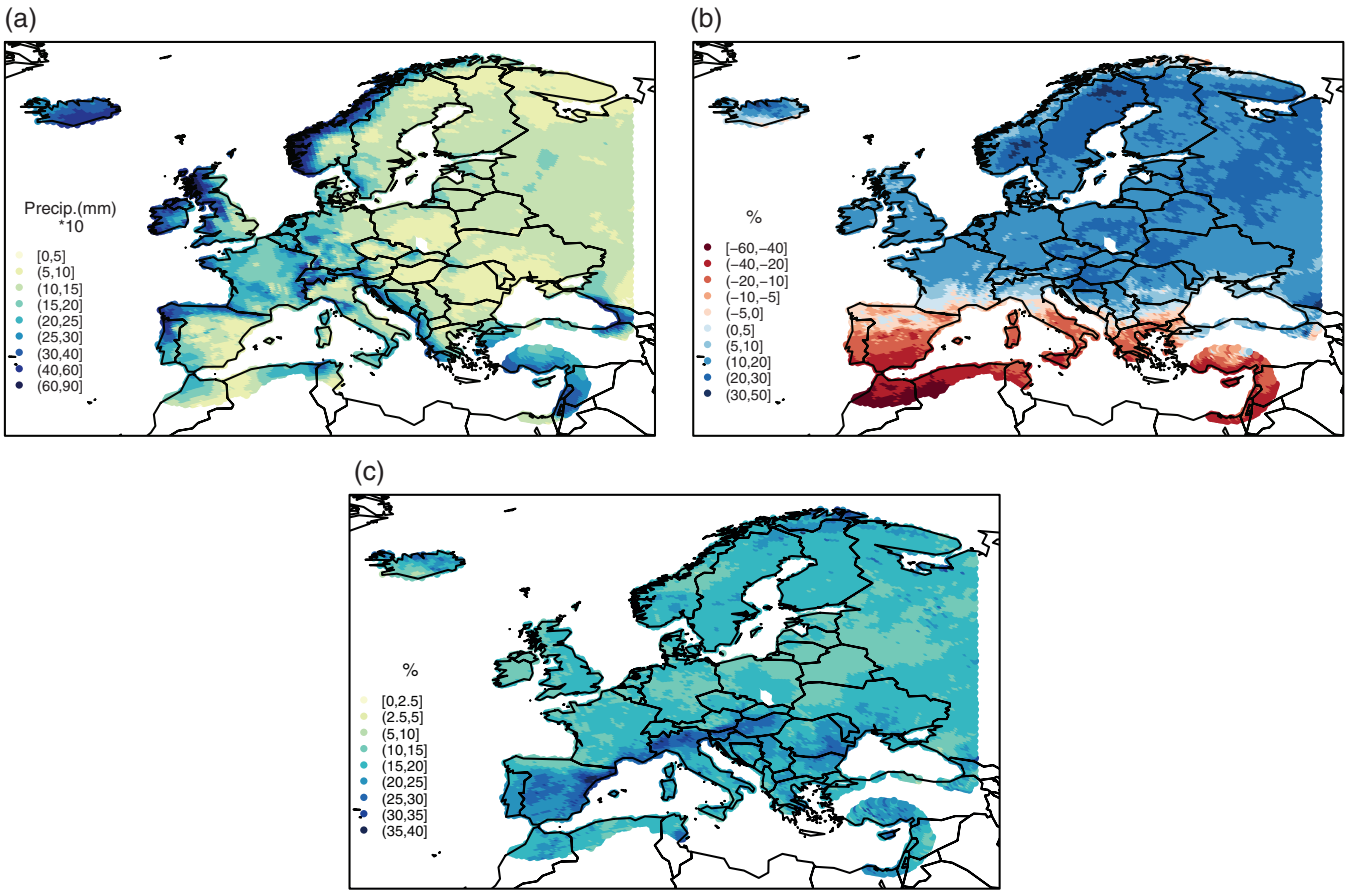

FIGURE 5 (a) Observed mean winter precipitation, (b) future change (in %, multi-model mean, 2071–2095, RCP8.5), and (c) the inter-model *SD* of the change (in %) [Colour figure can be viewed at wileyonlinelibrary.com]

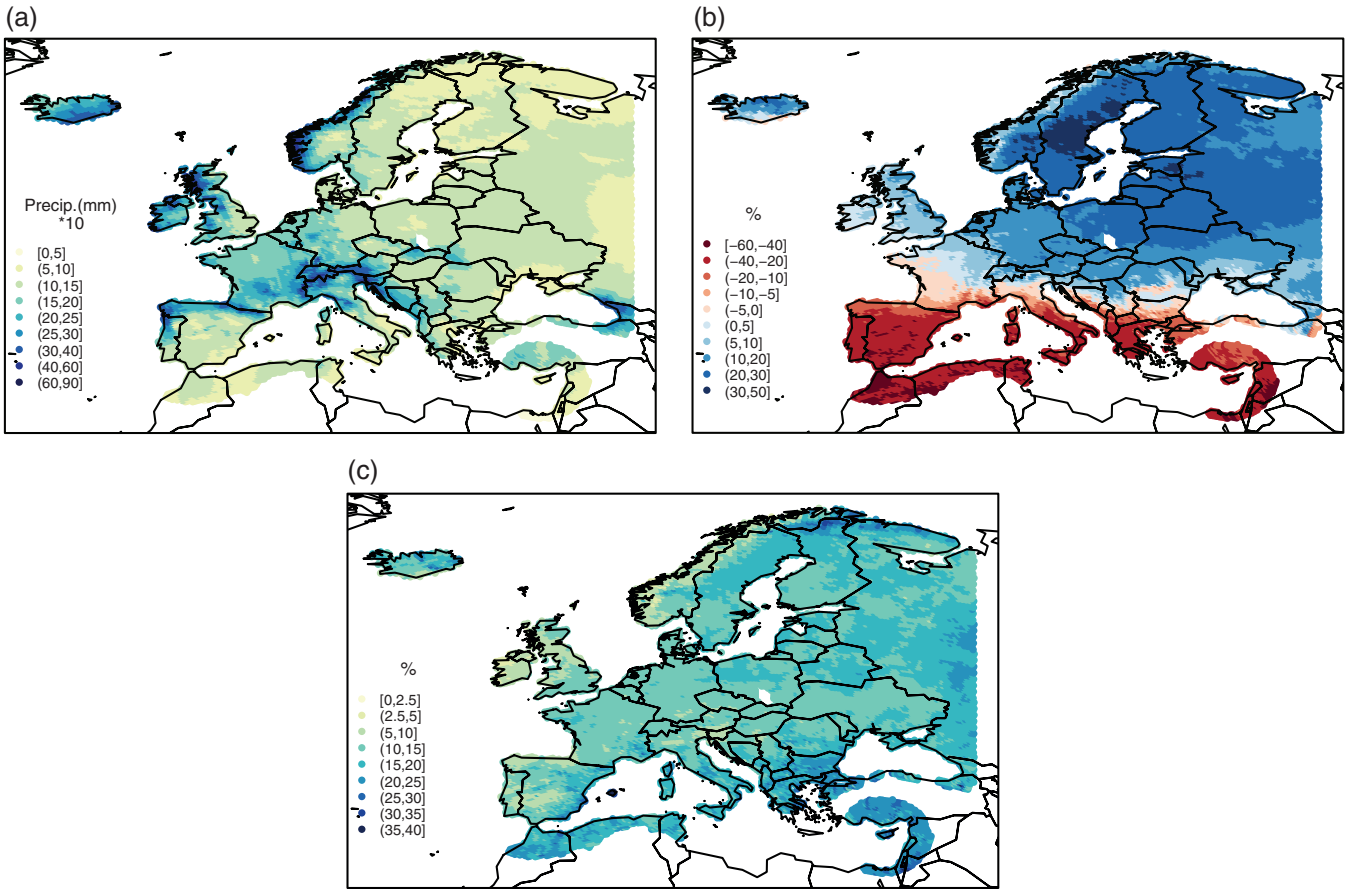

FIGURE 6 As in Figure 5, but for spring [Colour figure can be viewed at wileyonlinelibrary.com]

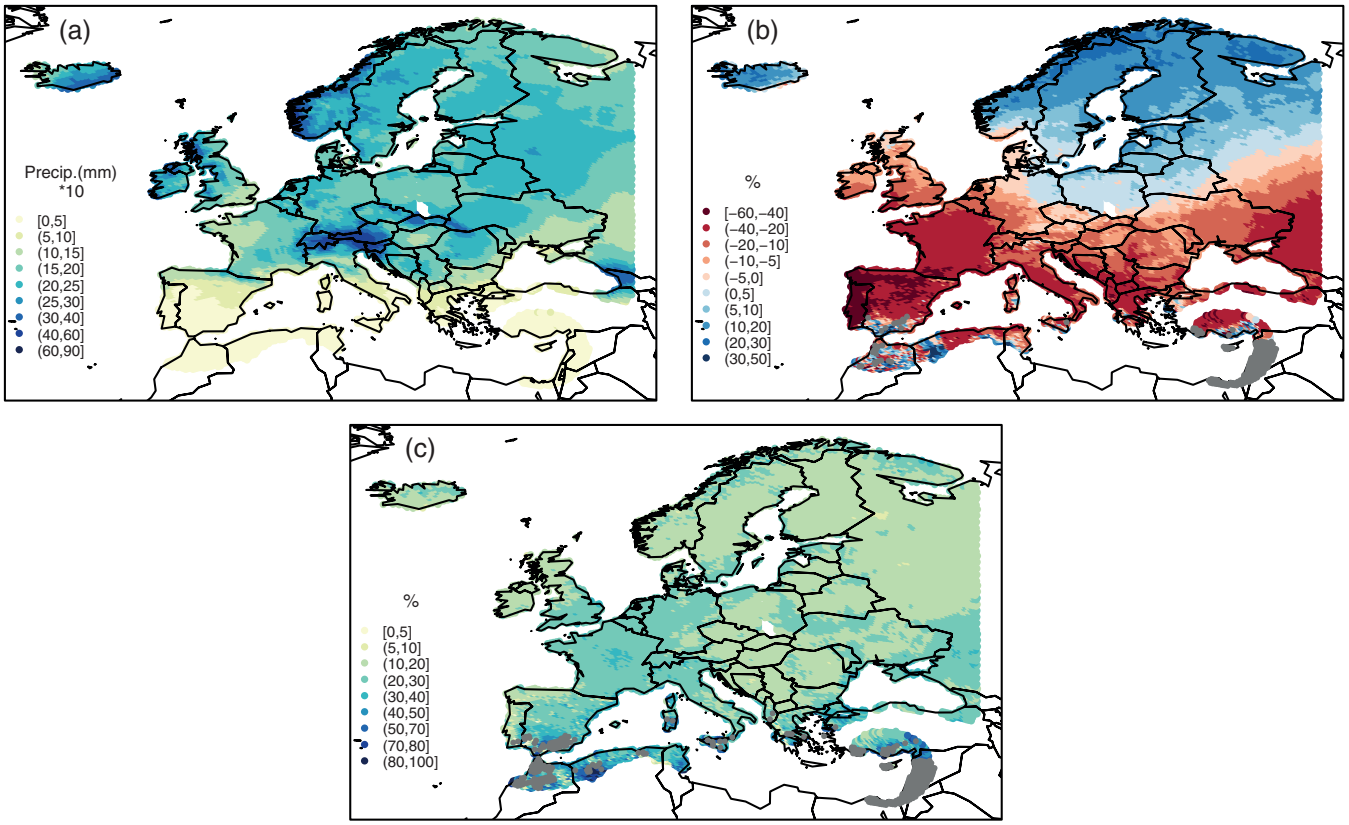

FIGURE 7 As in Figure 5, but for summer. Note that grey dots indicate precipitations <0.1 mm in (b) [Colour figure can be viewed at wileyonlinelibrary.com]

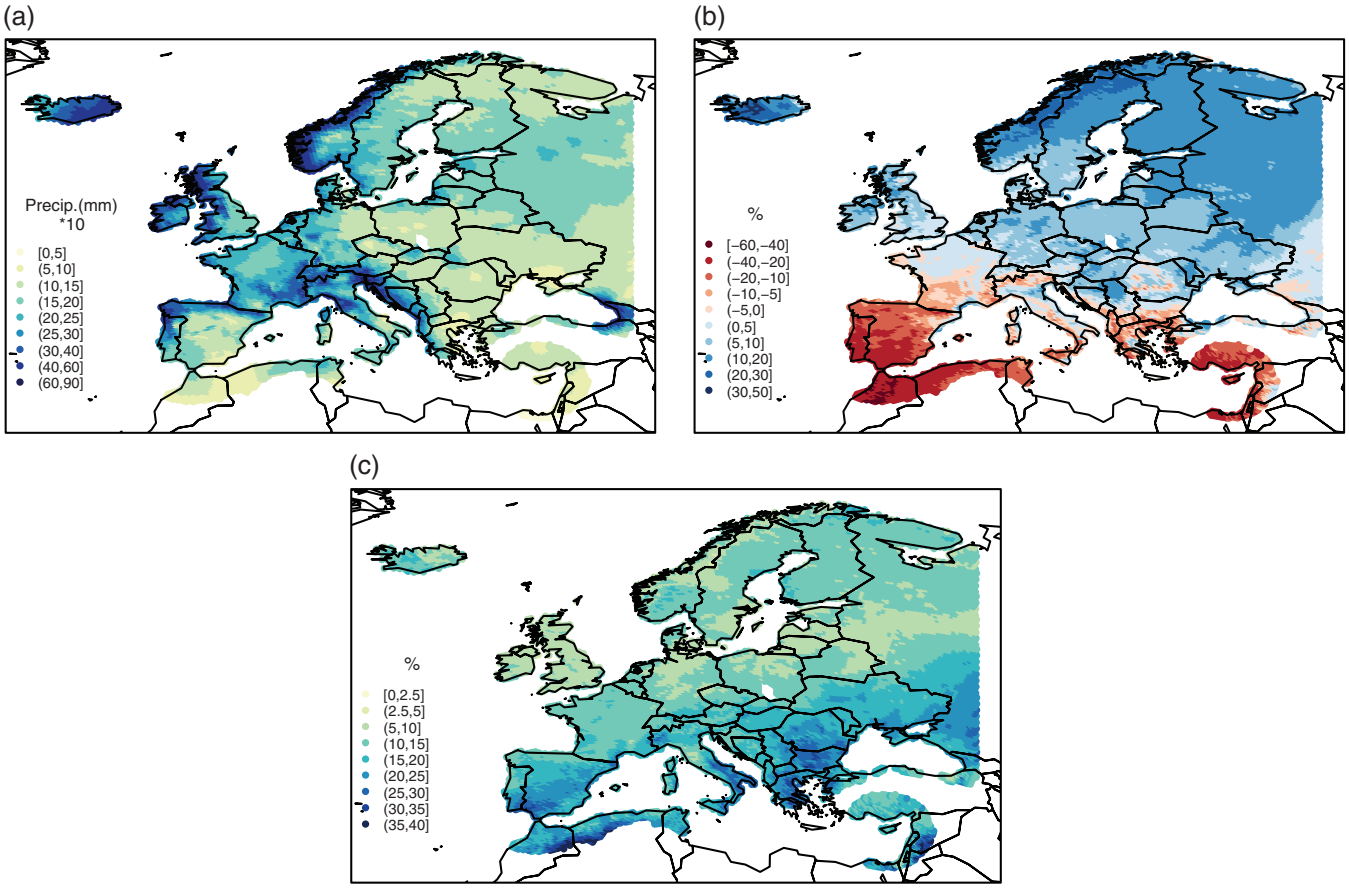

FIGURE 8 As in Figure 5, but for autumn [Colour figure can be viewed at wileyonlinelibrary.com]

overall decrease of precipitation in southern Europe and the Mediterranean (SEM) region can be expected during the late century (between −20 and −50%), while annual precipitation is supposed to increase in the north of Europe (Figure 3b). The pattern of the changes is very similar for RCP4.5, but less pronounced (not shown). Jacob *et al.* (2014) pointed out, using EURO-CORDEX RCP8.5 scenarios, a statistically significant rise in mean precipitation over large parts of central and northern Europe up to about 25%, and a decrease in southern Europe within the period 2071–2100 with respect to the present. Accordingly, the same substantial changes have been found but with increases up to 30% in the Nordic countries (NC) and decreases down to −50% in the south of the Iberian Peninsula (IP) and north of Africa (NA). Regarding the inter-model *SD* (Figure 3c), the maximum uncertainties are located in the SEM, probably because a large fraction of the annual rainfall is of convective nature. Also, note the important reduction of rainfall in the north of the IP (−20%) with a very high agreement among models (less than 12% in *SD*, Figure 3c).

Next, the future change in the annual number of precipitation days has been analysed. We define as precipitation days those in which daily values are in excess of 0.1 mm. With regard to the future change, there is an overall reduction in daily events except in north Europe, where a small rise is noted in the NC (up to +6%; Figure 4b). Models' uncertainties associated with these shifts are normally higher in the regions where the largest changes are found, and in those where convective rains represent a greater fraction of the total annual accumulated rainfall (Figure 4c).

Nevertheless, a significant decrease in the number of rainy days is observed in the central part of the IP and the south of France, with a high consensus among models. Since fewer annual precipitation days come in combination with a larger annual amounts over central Europe, an increase in mean daily precipitation can be expected in these zones.

3.2 | Future changes in seasonal regimes

3.2.1 | Precipitation

Regarding the projected seasonal trends, the change in mean annual precipitation at the end of the century would show an overall rise in central and northern Europe and a decrease in the SEM for all seasons, while the area of declining rainfall extends further north in summer. This dipole pattern is less pronounced under the RCP4.5 scenario. The observed mean precipitation, the multi-model mean projected changes and the associated standard deviation for the 2071–2095 period under that scenario, are depicted in Figures 5–8 for each season.

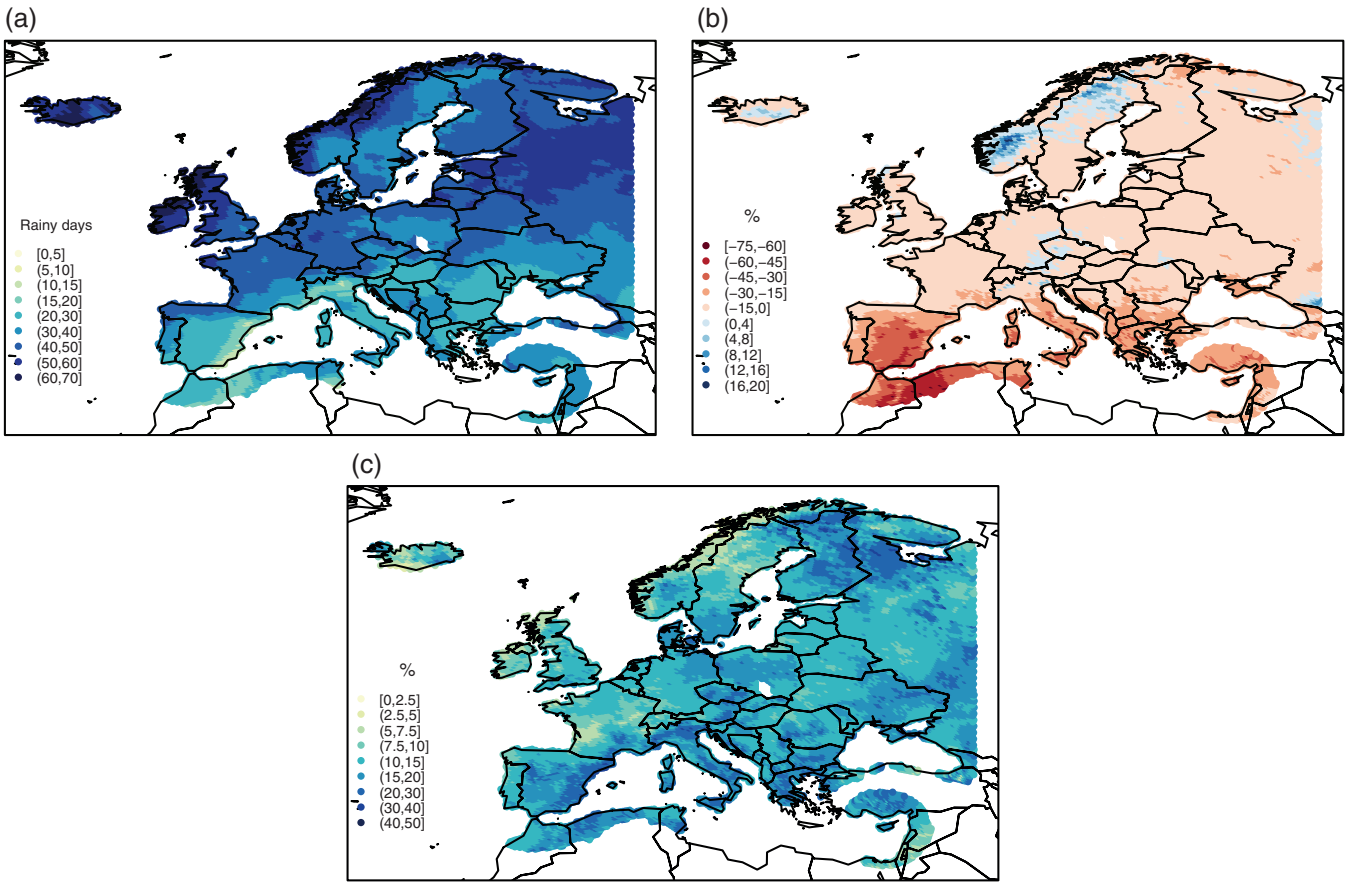

FIGURE 9 (a) Observed number of rainy days in winter, (b) future change (in %, multi-model mean, 2071–2095, RCP8.5), and (c) the inter-model *SD* of the change (in %) [Colour figure can be viewed at wileyonlinelibrary.com]

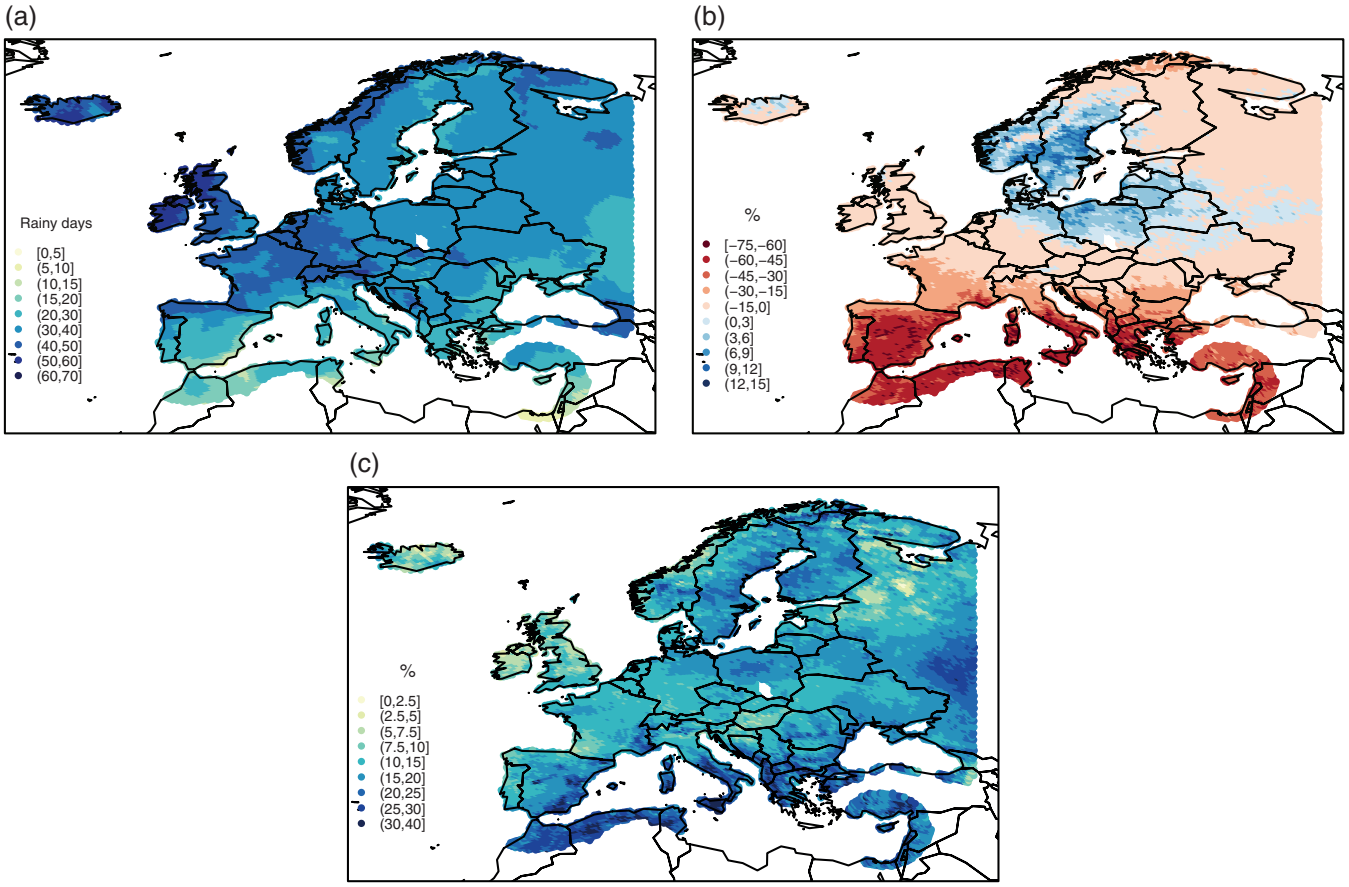

FIGURE 10 As in Figure 9, but for spring [Colour figure can be viewed at wileyonlinelibrary.com]

Jacob *et al*. (2014) pointed out that the zone between regions in which precipitation increases northern and decreases southern, shifts southwards in winter and northwards in summer by the end of the century. In our results, the precipitation increases in winter in the center, north, and southeast of Europe owing to the projected enhancement of Atlantic storm activity (Gao *et al*., 2006), with values up to approximately +30% in the NC and Russia. Then, it decreases in most of the Mediterranean, with more than 40% less rainfall in NA and a high consensus between models (Figure 5b,c). This reduction would be associated to a future rise of sea level pressure over the central Mediterranean in winter. Therefore, a climate with enhanced anticyclonic conditions would generally lead to greater stability and an environment less frequently conducive to storm generation (Giorgi and Lionello, 2008). The transition zone of precipitation between regions also shifts northwards in summer in the expected trends (Figure 7b). Nevertheless, these results depend on both the scenario emission and the time slice considered. For instance, mean winter precipitation would increase up to +10% in the north of the IP at the beginning of the century under the RCP4.5 scenario, with a very high certainty (not shown).

Concerning the spring contribution, the area of precipitation decrease expands further northwards to the extent of covering the entire Iberian, Italian, Balkan Peninsulas, as well as western France (Gao *et al*., 2006). A reduction of down to −20% is expected in the north of the IP, while precipitation will decrease up till −40% in the north of Morocco and south of Iberia. Note how the increments in the NC are more remarkable in this season, with the maximum positive signal of rainfall in Sweden (up to +30% Figure 6b). Percentage changes in precipitation amounts also present a high certainty for spring in the whole domain (Figure 6c).

In summertime, most of the European region, leaving out the northern part, shows a noticeable precipitation reduction (down to −50% in Portugal and north of the IP, Figure 7b). This fact has been attributed to the intensification of the anticyclonic ridge over the western Europe and northeastern Atlantic (Pal *et al*., 2004). It should be also noted that the projected changes in summer indicate, with a good confidence, an important decrease in the Alps and United Kingdom (−20%; Figure 7b,c).

The autumn contribution to the water resources is expected to decline in the Western and Eastern Mediterranean but not in the central part. The heterogeneous changes in the Mediterranean show a relevant decrease over Portugal, south of Iberia, and Turkey (−40%; Figure 8b). Regarding the positive signal of precipitation in the fall, it is also found a meaningful increase in the NC and Russia (up till +20%), with a very high confidence given the low inter-model *SD* (Figure 8c).

If we analyse the future change in the seasonal number of precipitation days, a significant decrease in the Mediterranean is found for all seasons, together with an increase in the NC (Figure 9b). The pattern of changes for the late century is very similar under the RCP4.5, but less pronounced (not shown). An important reduction up to −30% is obtained in the north of Russia and NC, except in summer. Nevertheless, the projected changes in the central, west, and northeast Europe has a different pattern depending on the season.

In winter, the results under the RCP8.5 indicate a positive change in the number of rainy days in some countries of central Europe (Czech Republic and Germany) and the NC (+20%; Figure 9b). Largest decreases will take place in the south of Spain and NA (down to −60%), with a good confidence in these results according to the low multi-model *SD* (Figure 9c). However, the future changes at the beginning of the century reveal a small positive signal in the north of Spain, France, and central Europe, being more remarkable for the RCP4.5 scenario.

Concerning the spring results, similar changes are found in the Mediterranean, but larger decreases have been obtained in the central part of Spain (down to −75%; Figure 10b). Similar decreasing trend is expected in the NA and south of Italy but with a low consensus among models (Figure 10c). The pattern of changes in the number of rainy days reveals a considerable increase in the north of Polonia and the south of the NC, but presents a low certainty in these results according to the low *SD*.

In summer, we can only await a small rise in the NC and the north of Russia (up to +20%), while it is observed an overall diminution in the rest of the domain (Figure 11b). It should be noted a decrease up till −100% in regions such as northwest of Africa, Turkey, south of Spain, and south of Italy, where it hardly rains more than 5 days in summer. An important diminution down to approximately −50% is also expected in the southern part of United Kingdom. Note that in this country currently rains more than 30 days per summer (Figure 11a) with mean seasonal amounts of 200 mm. The change in the number of summer precipitation days exhibits good agreement among models in the SEM and northern Europe (Figure 11c).

In autumn, the projections only show a slight rise in Norway and Iceland, with medium agreement among models (Figure 12b,c). However, the same reduction pattern found in summer is observed in United Kingdom, northern Spain, France, and Italy, with a lower percentage of decrease (−30%) and a high certainty as measured by the inter-model differences. Finally, it is meaningful that the largest diminutions in the number of rainy days in autumn will occur in the central part of Spain, NA, and Turkey, as in spring and summer.

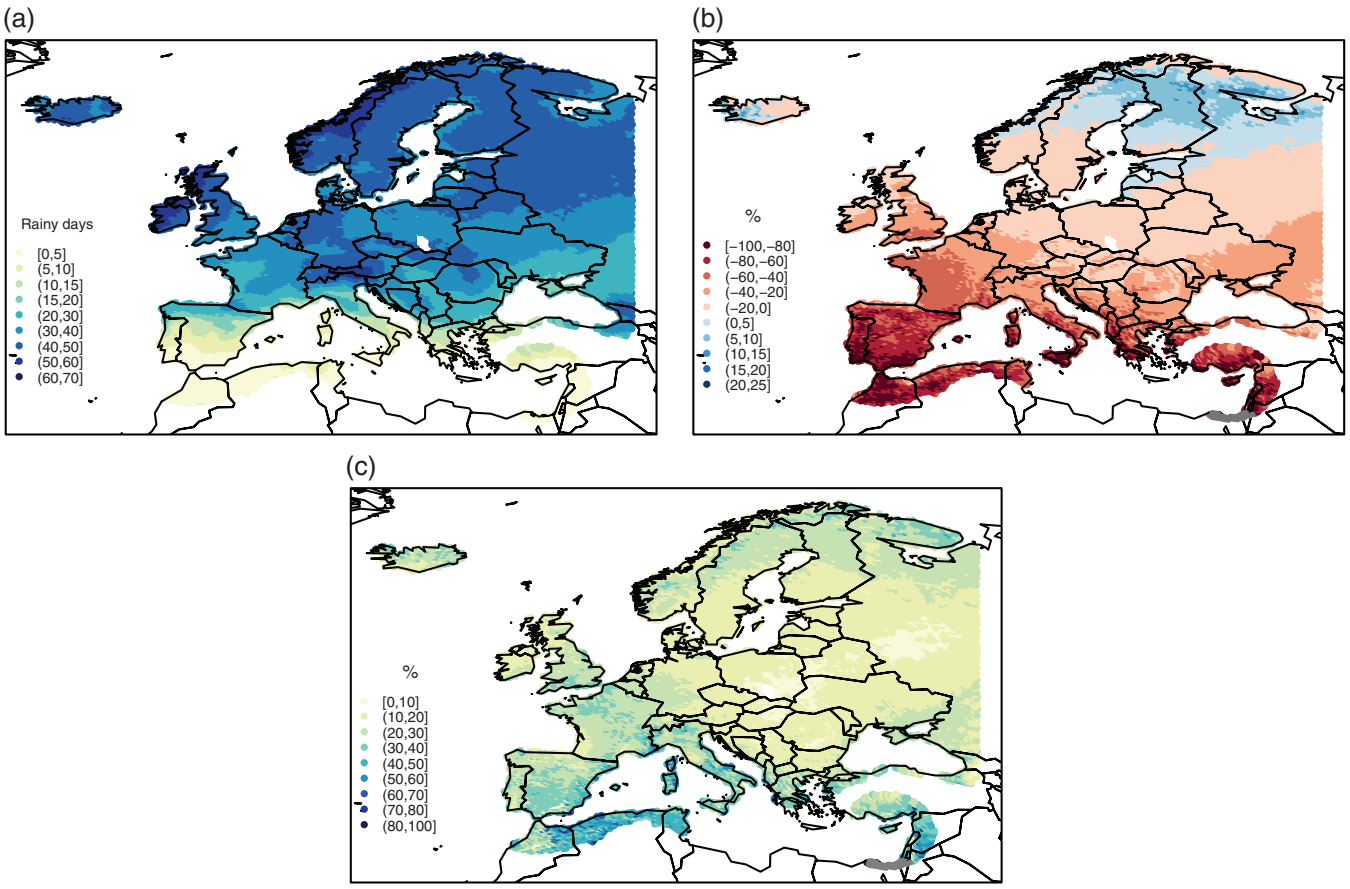

FIGURE 11 As in Figure 9, but for summer. Note that grey dots indicate precipitations <0.1 mm in (b) [Colour figure can be viewed at wileyonlinelibrary.com]

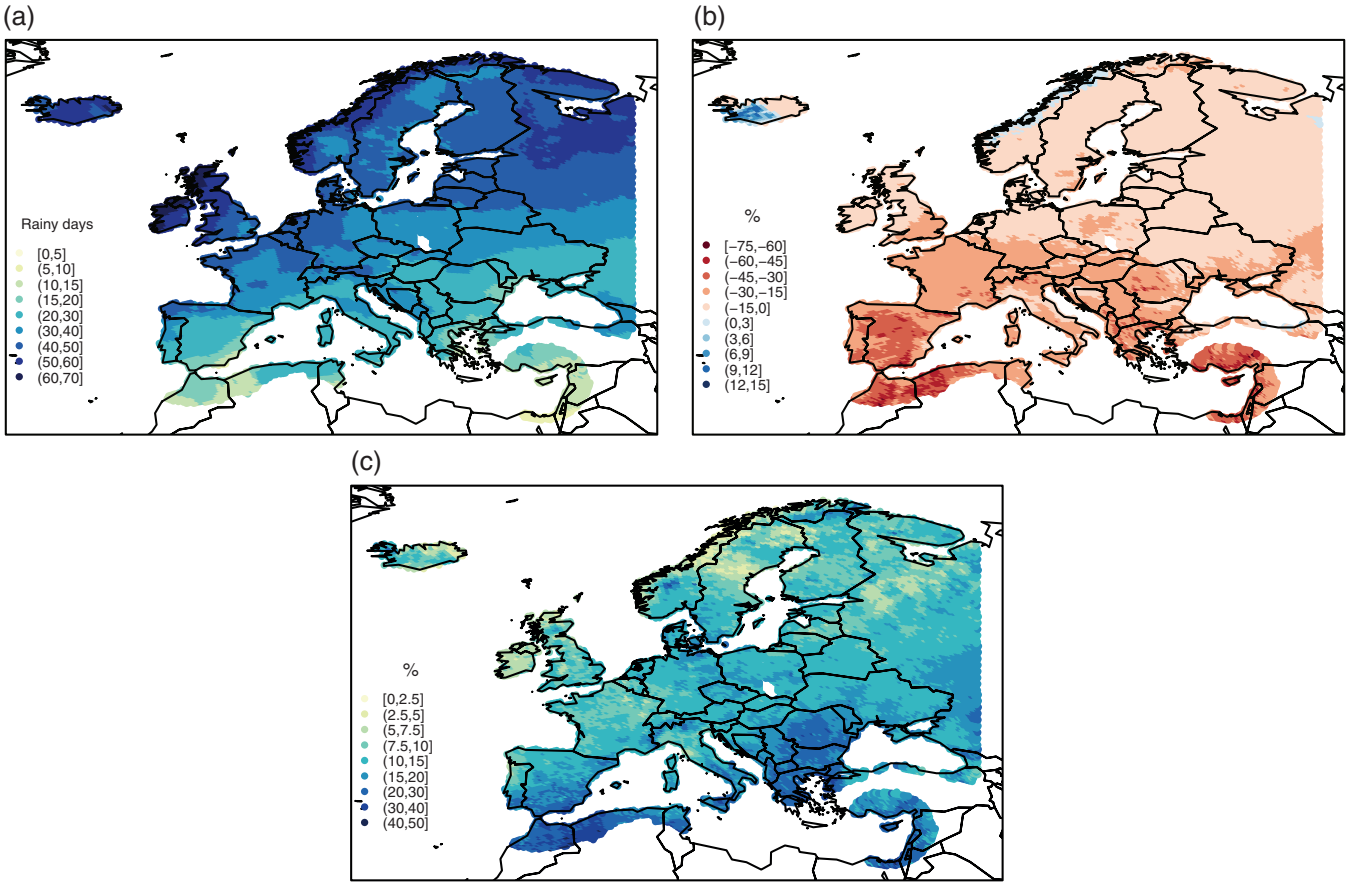

FIGURE 12 As in Figure 9, but for autumn [Colour figure can be viewed at wileyonlinelibrary.com]

3.2.2 | Temperature

With regard to the projected seasonal results for temperature, the change in mean regimes would evidence an overall rise of the minimum temperature for all seasons at the end of the century, being more remarkable in summer and autumn for the Mediterranean (up to 6.5 and 5°C, respectively, for the late 21st century; Figure 13e,g). Winter and spring projections reveal the largest increases in north Europe, at least partially in response to reduced snow cover there (Giorgi and Lionello, 2008). The pattern of changes is very much alike under the RCP4.5 scenario but less pronounced (not shown).

In winter, the projected changes of minimum temperature show increases between 2 and 3.5 °C in the SEM and United Kingdom, while a significant rise is expected in northwestern Spain, the Alps, and Turkey (4.5 °C; Figure 13a). The multi-model mean also projects a positive signal in central and northern Europe that ranges from 2.5 to 5 °C and from 5 to 8 °C, respectively, with higher uncertainty the greater are the expected multi-model mean changes (Figure 13b).

The same warming geographical pattern has been identified in spring, except in central Europe, where the positive changes only reach 4 °C, and in the Mediterranean, where notable increases up to 4 °C are also detected in south Spain and the NA (Figure 13c).

In summertime, the projections point out the largest increases in the SEM and the lowest in central and north Europe. It is also noticeable that the most positive changes in SEM are revealed in the center of Spain and Turkey (up to 6.5 °C; Figure 13e), with a robust agreement among models (less than 1.25 °C in *SD*; Figure 13f).

However, the multi-model mean in autumn projects a different geographical warming pattern, being more marked in north Europe and the Mediterranean and less pronounced in United Kingdom and central Europe (between 2.5 and 4 °C; Figure 13g).

The pattern of warming for the maximum temperatures is very similar to that of the minimum temperature for all seasons, but showing larger increases in all the domain. Therefore, we also expect an overall rise under the RCP8.5 scenario, being more pronounced in the Mediterranean for spring, summer, and autumn (up to 6.5, 8, and 5 °C, respectively; at the end of the century, Figure 14c,e,g). The seasonal maximum temperatures in winter and spring show again the largest growth rate in the northern countries and Turkey, albeit with low certainty attending to the large inter-model *SD* in the signal (more than 2 °C in *SD*; Figure 14b,d).

Nevertheless, future projections of maximum temperature in United Kingdom and the western Mediterranean present increases between 2 and 4 °C, with a very high consensus among models, being the positive signal more remarkable for spring (Figure 14c). A steady rise of the maximum temperature in summer is identified from north to south of Europe,

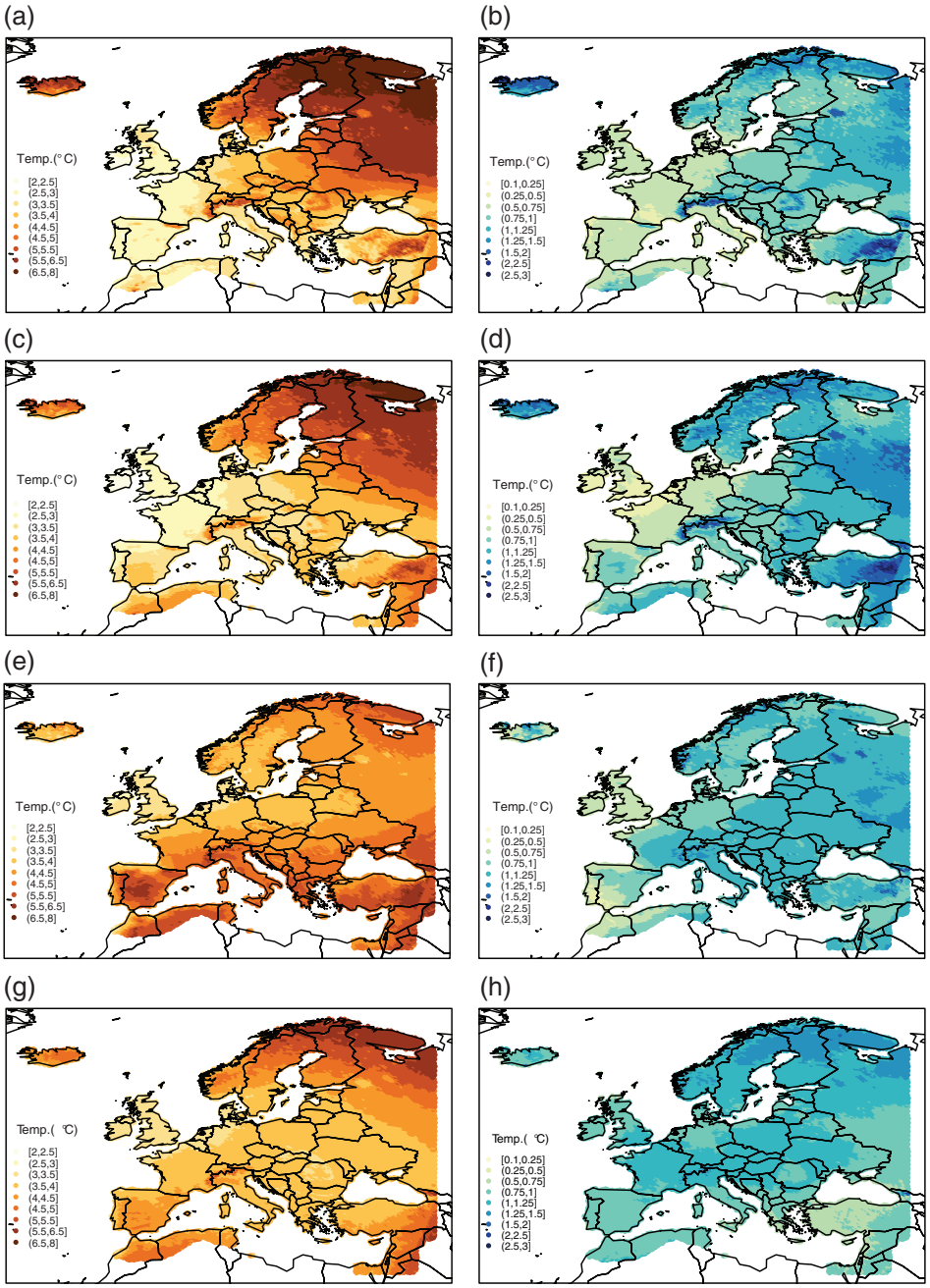

FIGURE 13 Future change of minimum temperature (in °C, multi-model mean, 2071–2095, RCP8.5) and inter-model *SD* of the change for: winter (a, b), spring (c, d), summer (e, f), and autumn (g, h) [Colour figure can be viewed at wileyonlinelibrary.com]

with the highest growth rate in Turkey, NA, and south of Spain (up to 6.5, 8, and 6.5 °C, respectively; Figure 14e). Mind also the significant change of maximum temperature over these regions for the last decades of the century in the fall, with a rise up to 5 °C and a high certainty as measured by the inter-model differences (Figure 14g,h).

4 | CONCLUSIONS AND FURTHER REMARKS

A study of the future changes in temperature and precipitation at annual and seasonal scales over Europe has been carried out in this work. The assessment of climate change impacts and the identification of the most vulnerable zones of the continent is an issue of major concern. Availability of quantitative projections should be considered a useful tool to European policy makers and stakeholders to enhance their capacity to respond more effectively to the impacts of climate change at local, regional, national, and continental levels. For these purposes, observed and simulated daily series of 2-m minimum and maximum temperatures and precipitation have been analysed. For the future projections, several RCMs from the EURO-CORDEX project have been used to deal with the uncertainties arising from the model errors and the imperfect GCM-derived boundary conditions.

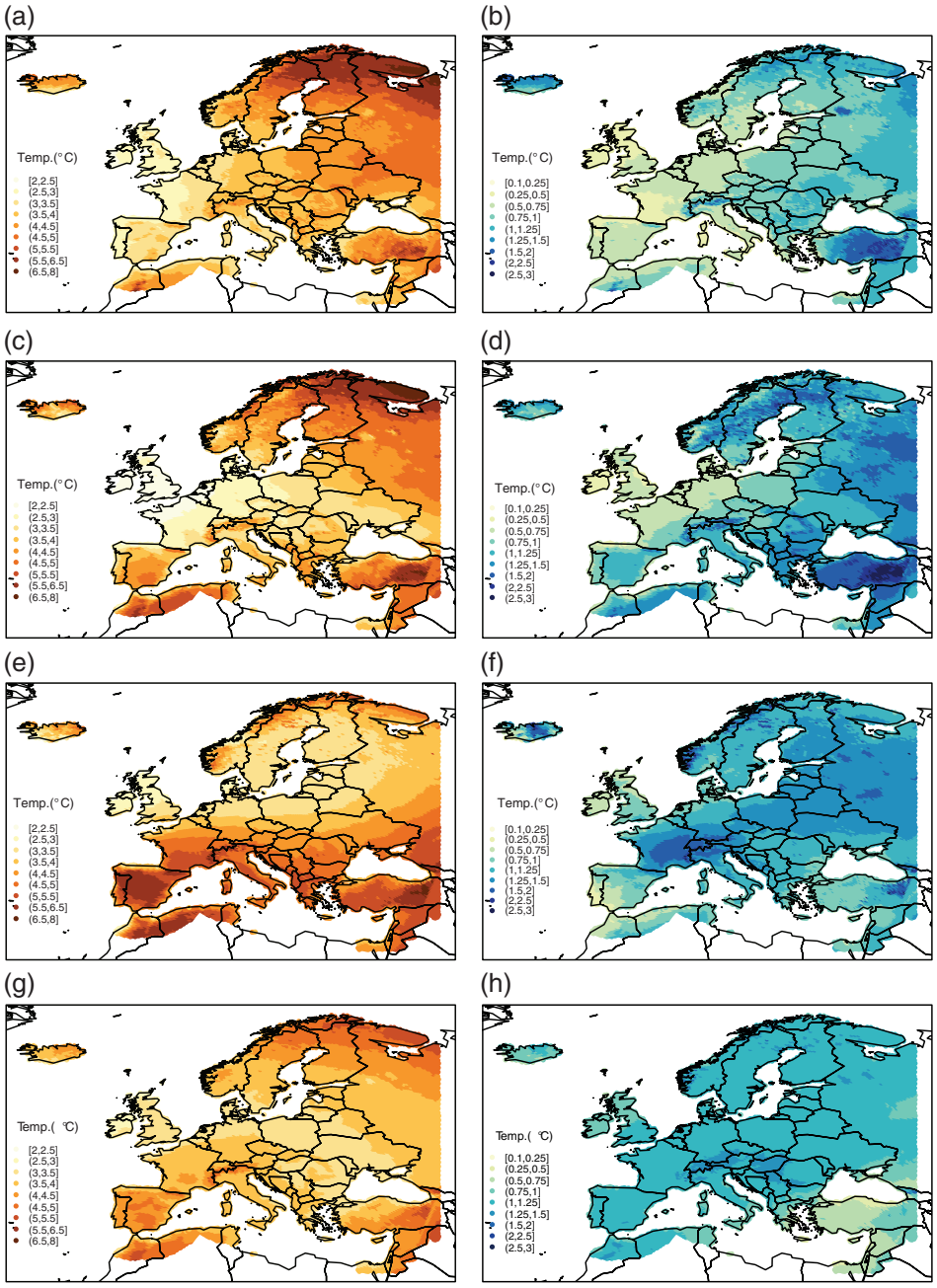

FIGURE 14 As in Figure 13 but for maximum temperature [Colour figure can be viewed at wileyonlinelibrary.com]

Simulations using the RCP4.5 and RCP8.5 scenarios have been considered. Results from RCP8.5 (a high emission scenario) have been analysed and presented in detail.

We have developed a modification of the quantile–quantile adjustment, previously presented in Amengual *et al.* (2012), in order to alleviate RCMs' outputs biases. The skill of the *global* and *local* adjustments has been checked for two different 25-year validation periods. Our modified quantile–quantile adjustment focus on better handling the statistical distribution of extremes. First, the verification has been carried out for a *continuous* 1956–1980 period, annually and seasonally, to better assess the advantages of using the technique. Second, a verification of the method for a period of 25 *alternate* years (from 1956 to 2005) has been performed in order to isolate the effects of the climate change signal on the training of the adjustment method.

Results show an overall improvement in reproducing the present climate (e.g., 1956–1980) when using calibrated series instead of raw RCM outputs, as well as the benefits of the *local* adjustment compared to the "*global* calibrated" RCM outputs. Specifically, the application of the *local* approach clearly reduces the errors found in the statistical distributions of the extreme values. The validation with *alternate* years also reveals a general improvement when the Q–Q adjustment is used, and the results are even better than those for the *continuous* validation period (1956–1980). Nevertheless, the PSS ensemble mean of the whole PDFs does not exhibit a clear improvement for daily precipitation when applying the statistical correction.

Once RCM daily series were calibrated against the European observational database, the projected climate change signal has been analysed. The signal has been discussed in terms of changes in annual and seasonal mean regimes at the end of the 21st century. A significant warming has been obtained for all seasons and the entire Europe, being more marked in the Mediterranean for summers and autumns with a high level of confidence, as measured by the amplitude of inter-model *SD*. The highest increments of minimum and maximum temperatures in summer occur in central Spain and Turkey, with values of up to 6.5 and 8 °C, respectively. In winter and spring, the largest positive changes are expected in northern Europe (above 6.5 and 5.5 °C, respectively) with higher uncertainty range associated with the inter-model differences. However, in terms of magnitude, the inter-model *SD* is generally quite small compared with the multi-model average warming signals, confirming the robustness of the obtained temperature tendencies.

Prospects on future annual and seasonal changes in precipitation are more variable across the different European subregions. Annual changes show an overall decrease in SEM during the late 21st century, while in north Europe the precipitation is expected to increase. In addition, a general diminution in the number of annual precipitation days is projected, except for north Europe where an important rise has been observed (+30%). Therefore, an increase in mean daily precipitation intensities over central Europe is expected, as there will be less annual precipitation days but a positive change in mean annual rainfall.

Regarding the projected seasonal regimes in precipitation, the results reveal an overall rise in central and northern Europe and a decrease in the SEM for all seasons, while the area of declining rainfall extends further north in summer. This dipole pattern is less pronounced under the RCP4.5 scenario. Finally, it is also detected a significant reduction in the number of annual precipitation days in the Mediterranean for all seasons, while in the NC and the north-west part of Russia is expected to increase. A significant decrease of down to −30% is also obtained in the northern sector of Russia and the NC, except in summer. Nevertheless, the projected tendencies in central, west and northeast Europe depicts a different geographical pattern of average rainfall depending on the season. Additionally, the multi-model *SD* of annual and seasonal precipitation is generally smaller than the mean signal by the late century.

Changes in many extreme weather events (e.g., heat waves, persistent droughts, heavy precipitation, severe convective storms, etc.) have been observed since about 1950. It is very likely that the number of cold days and nights has decreased and the number of warm days and nights has increased on the global scale. In addition, there are likely more land regions where the number of heavy precipitation events has increased than where it has decreased (Stocker *et al*., 2013). In future work, we plan to exploit these daily precipitation and temperature projections to analyse in detail the future changes in extreme weather events over Europe. Recall that extreme events are responsible for most of natural, human and economic costs in many European regions, including the Mediterranean zone.

ACKNOWLEDGEMENTS

This research is framed within the CGL2014-52199-R (Future Regional Impacts of Climate Change Associated to Extreme Weather Phenomena [EXTREMO]) Spanish project which is partially supported with AEI/FEDER funds. The first author was also supported by the FPI-CAIB (FPI/1931/2016) grant from the Conselleria d'Innovació, Recerca i Turisme del Govern de les Illes Balears and the Fons Social Europeu. The authors acknowledge the EURO-CORDEX project, sponsored by the World Climate Research Program (WRCP). The E-OBS data set from the EU-FP6 project and data providers in the ECA and D project (eca.knmi.nl) are also acknowledged.

ORCID

M.F. Cardell https://orcid.org/0000-0002-8856-8666

REFERENCES

Ahmed, K.F., Wang, G., Silander, J., Wilson, A.M., Allen, J.M., Horton, R. and Anyah, R. (2013) Statistical downscaling and bias correction of climate model outputs for climate change impact assessment in the US northeast. *Global and Planetary Change*, 100, 320–332. https://doi.org/10.1016/j.gloplacha.2012.11.003.

Amengual, A., Homar, V., Romero, R., Alonso, S. and Ramis, C. (2012) A statistical adjustment of regional climate model outputs to local scales: application to Platja de Palma, Spain. *Journal of Climate*, 25(3), 939–957. https://doi.org/10.1175/JCLI-D-10-05024.1.

Boé, J., Terray, L., Habets, F. and Martin, E. (2007) Statistical and dynamical downscaling of the Seine Basin climate for hydro-meteorological studies. *International Journal of Climatology*, 27(12), 1643–1655. https://doi.org/10.1002/joc.1602.

Cannon, A.J., Sobie, S.R. and Murdock, T.Q. (2015) Bias correction of GCM precipitation by quantile mapping: How well do methods preserve changes in quantiles and extremes? *Journal of Climate*, 28(17), 6938–6959.

Christensen, J.H. and Christensen, O.B. (2007) A summary of the prudence model projections of changes in European climate by the end of this century. *Climatic Change*, 81(1), 7–30. https://doi.org/10.1007/s10584-006-9210-7.

Déqué, M. (2007) Frequency of precipitation and temperature extremes over France in an anthropogenic scenario: model results and statistical correction according to observed values. *Global and Planetary Change*, 57(1–2), 16–26. https://doi.org/10.1016/j.gloplacha.2006.11.030.

Dobler, A. and Ahrens, B. (2008) Precipitation by a regional climate model and bias correction in Europe and South Asia. *Meteorologische Zeitschrift*, 17(4), 499–509. https://doi.org/10.1127/0941-2948/2008/0306.

Gao, X., Pal, J.S. and Giorgi, F. (2006) Projected changes in mean and extreme precipitation over the mediterranean region from a high resolution double nested RCM simulation. *Geophysical Research Letters*, 33(3), L03706. https://doi.org/10.1029/2005GL024954.

Giorgi, F. (2006) Climate change hot-spots. *Geophysical Research Letters*, 33, 1–4. https://doi.org/10.1029/2006GL025734.

Giorgi, F. and Lionello, P. (2008) Climate change projections for the mediterranean region. *Global and Planetary Change*, 63(2–3), 90–104. https://doi.org/10.1016/j.gloplacha.2007.09.005.

Giorgi, F. and Mearns, L.O. (1999) Introduction to special section: regional climate modeling revisited. *Journal of Geophysical Research: Atmospheres*, 104(D6), 6335–6352. https://doi.org/10.1029/98JD02072.

Giorgi, F., Jones, C. and Asrar, G.R. (2009) Addressing climate information needs at the regional level: the cordex framework. *World Meteorological Organization (WMO) Bulletin*, 58(3), 175–183.

Goodess, C.M., Anagnostopoulo, C., Bárdossy, A., Frei, C., Harpham, C., Haylock, M.R., Hundecha, Y., Maheras, P., Ribalaygua, J., Schmidli, J., Schmith, T., Tolika, K., Tomozeiu, R. and Wilby, R.L. (2012) *An intercomparison of statistical downscaling methods for Europe and European regions – assessing their performance with respect to extreme temperature and precipitation events*. Norwich: Climatic Research Unit Research Publication (CRURP), University of East Anglia. Available at: http://www.cru.uea.ac.uk/cru/pubs/crurp/CRU_RP11.pdf [Accessed 1st January 2012].

Haylock, M., Hofstra, N., Klein Tank, A., Klok, E., Jones, P. and New, M. (2008) A European daily high-resolution gridded data set of surface temperature and precipitation for 1950–2006. *Journal of Geophysical Research: Atmospheres*, 113(D20), D20119. https://doi.org/10.1029/2008JD010201.

Herrera, S., Fernández, J. and Gutiérrez, J. (2016) Update of the spain02 gridded observational dataset for EURO-CORDEX evaluation: assessing the effect of the interpolation methodology. *International Journal of Climatology*, 36(2), 900–908. https://doi.org/10.1002/joc.4391.

Ivanov, M.A. and Kotlarski, S. (2017) Assessing distribution-based climate model bias correction methods over an alpine domain: added value and limitations. *International Journal of Climatology*, 37(5), 2633–2653.

Ivanov, M.A., Luterbacher, J. and Kotlarski, S. (2018) Climate model biases and modification of the climate change signal by intensity-dependent bias correction. *Journal of Climate*, 31(16), 6591–6610.

Jacob, D., Petersen, J., Eggert, B., Alias, A., Christensen, O.B., Bouwer, L.M., Braun, A., Colette, A., Déqué, M., Georgievski, G., Georgopoulou, E., Gobiet, A., Menut, L., Nikulin, G., Haensler, A., Hempelmann, N., Jones, C., Keuler, K., Kovats, S., Kröner, N., Kotlarski, S., Kriegsmann, A., Martin, E., van Mei-jgaard, E., Moseley, C., Pfeifer, S., Preuschmann, S., Radermacher, C., Radtke, K., Rechid, D., Rounsevell, M., Samuelsson, P., Somot, S., Soussana, J.-F., Teichmann, C., Valentini, R., Vau-tard, R., Weber, B. and Yiou, P. (2014) EURO-CORDEX: new high-resolution climate change projections for European impact research. *Regional Environmental Change*, 14 (2), 563–578. https://doi.org/10.1007/s10113-013-0499-2.

Johnson, F. and Sharma, A. (2012) A nesting model for bias correction of variability at multiple time scales in general circulation model precipitation simulations. *Water Resources Research*, 48(1), W01504. https://doi.org/10.1029/2011WR010464.

Kotlarski, S., Keuler, K., Christensen, O.B., Colette, A., Deque, M., Gobiet, A., Goergen, K., Jacob, D., Luethi, D., Van Meijgaard, E., Nikulin, G., Schaer, C., Teichmann, C., Vautard, R., Warrach-Sagi, K. and Wulfmeyer, V. (2014) Regional climate modeling on European scales: a joint standard evaluation of the EURO-CORDEX RCM ensemble. *Geoscientific Model Development*, 7(4), 1297–1333. https://doi.org/10.5194/gmd-7-1297-2014.

Kotlarski, S., Szabó, P., Herrera, S., Räty, O.E., Keuler, K., Soares, P.M., Cardoso, R.M., Bosshard, T., Pagé, C., Boberg, F., Gutiérrez, J.M., Isotta, F. A., Jaczewski, A., Kreienkamp, F., Liniger, M.A., Lussana, C. and Pianko-Kluczyńska, K. (2017) Observational uncertainty and regional climate model evaluation: a pan-European perspective. *International Journal of Climatology*. https://doi.org/10.1002/joc.5249.

Maraun, D., Shepherd, T.G., Widmann, M., Zappa, G., Walton, D., Gutiérrez, J., Hagemann, S., Richter, I., Soares, P.M., Hall, A. and Mearns, L.O. (2017) Towards process-informed bias correction of climate change simulations. *Nature Climate Change*, 7(11), 764–773.

Meinshausen, M., Smith, S.J., Calvin, K.V., Daniel, J.S., Kainuma, J.F., Lamarque, M., Matsumoto, K., Montzka, S.A., Raper, S.C.B., Riahi, K., Thomson, A.M., Velders, G.J.M. and van Vuuren, D. (2011) The RCP greenhouse gas concentrations and their extensions from 1765 to 2300. *Climatic Change*, 109(1–2), 213. https://doi.org/10.1007/s10584-011-0156-z.

Moss, R., Babiker, M., Brinkman, S., Calvo, E., Carter, T.R., Edmonds, J., Elgizouli, I., Emori, S., Erda, L., Hibbard, K., Jones, R., Kainuma, M., Kelleher, J., Lamarque, J.-F., Manning, M.R., Matthews, B., Meehl, J., Meyer, L., Mitchell, J.F.B., Nakicenovic, N., O'Neill, B., Pichs, R., Riahi, K., Rose, S. K., Runci, P., Stouffer, R.J., van Vuuren, D.P., Weyant, J.P., Wilbanks, T.J., van Ypersele, J.P. and Zurek M. (2008) *Towards New Scenarios for the Analysis of Emissions, Climate Change, Impacts and Response Strategies*. Geneva: Intergovernmental Panel on Climate Change, 132 pp.

Pal, J.S., Giorgi, F. and Bi, X. (2004) Consistency of recent European summer precipitation trends and extremes with future regional climate projections. *Geophysical Research Letters*, 31(13), L13202. https://doi.org/10.1029/2004GL019836.

Perkins, S., Pitman, A., Holbrook, N. and McAneney, J. (2007) Evaluation of the ar4 climate models' simulated daily maximum temperature, minimum temperature, and precipitation over Australia using probability density functions. *Journal of Climate*, 20(17), 4356–4376. https://doi.org/10.1175/JCLI4253.1.

Piani, C., Haerter, J. and Coppola, E. (2010) Statistical bias correction for daily precipitation in regional climate models over europe. *Theoretical and Applied Climatology*, 99(1–2), 187–192. https://doi.org/10.1007/s00704-009-0134-9.

Reichle, R.H. and Koster, R.D. (2004) Bias reduction in short records of satellite soil moisture. *Geophysical Research Letters*, 31(19), L19501. https://doi.org/10.1029/2004GL020938.

Schär, C., Ban, N., Fischer, E.M., Rajczak, J., Schmidli, J., Frei, C., Giorgi, F., Karl, T.R., Kendon, E.J., Tank, A.M.G.K., O'Gorman, P.A., Sillmann, J., Zhang, X. and Zwiers, F.W. (2016) Percentile indices for assessing changes in heavy precipitation events. *Climatic Change*, 137(1), 201–216.

Štěpánek, P., Zahradníček, P., Farda, A., Skalák, P., Trnka, M., Meitner, J. and Rajdl, K. (2016) Projection of drought-inducing climate conditions in The Czech Republic according to EURO-CORDEX models. *Climate Research*, 70(2–3), 179–193. https://doi.org/10.3354/cr01424.

Stocker, T., Qin, D., Plattner, G., Tignor, M., Allen, S., Boschung, J., Nauels, A., Xia, Y., Bex, V. and Midgley, P. (2013) *IPCC 2013: Climate Change 2013: The Physical Science Basis. Contribution of Working Group I to the Fifth Assessment Report of the Intergovernmental Panel on Climate Change*. Geneva: IPCC, 1535 pp.

Suh, M.-S., Oh, S.-G., Lee, D.-K., Cha, D.-H., Choi, S.-J., Jin, C.-S. and Hong, S.-Y. (2012) Development of new ensemble methods based on the performance skills of regional climate models over South Korea. *Journal of Climate*, 25(20), 7067–7082. https://doi.org/10.1175/JCLI-D-11-00457.1.

Teutschbein, C. and Seibert, J. (2012) Bias correction of regional climate model simulations for hydrological climate-change impact studies: review and evaluation of different methods. *Journal of Hydrology*, 456, 12–29. https://doi.org/10.1016/j.jhydrol.2012.05.052.

Themeßl, M.J., Gobiet, A. and Heinrich, G. (2012) Empirical–statistical downscaling and error correction of regional climate models and its impact on the climate change signal. *Climatic Change*, 112(2), 449–468. https://doi.org/10.1002/joc.2168.

Tramblay, Y., Ruelland, D., Somot, S., Bouaicha, R. and Servat, E. (2013) High-resolution MED-CORDEX regional climate model simulations for hydrological impact studies: a first evaluation of the ALADIN-climate model in Morocco. *Hydrology and Earth System Sciences*, 17(10), 3721–3739.

Van der Linden, P. and Mitchell, J. (2009) *Ensembles: climate change and its impacts: summary of research and results from the ensembles project*. Exeter: Met Office Hadley Centre, p. 160.

Vrac, M. (2018) Multivariate bias adjustment of high-dimensional climate simulations: the rank resampling for distributions and dependences (r 2 d 2) bias correction. *Hydrology and Earth System Sciences*, 22(6), 3175.

Vrac, M., Noël, T. and Vautard, R. (2016) Bias correction of precipitation through singularity stochastic removal: because occurrences matter. *Journal of Geophysical Research: Atmospheres*, 121(10), 5237–5258.

Wang, Y., Leung, L.R., McGREGOR, J.L., Lee, D.-K., Wang, W.-C., Ding, Y. and Kimura, F. (2004) Regional climate modeling: progress, challenges, and prospects. *Journal of the Meteorological Society of Japan, Series II*, 82(6), 1599–1628. https://doi.org/10.2151/jmsj.82.1599.

Wood, A.W., Leung, L.R., Sridhar, V. and Lettenmaier, D. (2004) Hydrologic implications of dynamical and statistical approaches to downscaling climate model outputs. *Climatic Change*, 62(1–3), 189–216. https://doi.org/10.1023/B:CLIM.0000013685.99609.9e.

How to cite this article: Cardell MF, Romero R, Amengual A, Homar V, Ramis C. A quantile–quantile adjustment of the EURO-CORDEX projections for temperatures and precipitation. *Int J Climatol*. 2019; 39:2901–2918. https://doi.org/10.1002/joc.5991